



## **Stock assessment**

### **Falkland calamari (*Doryteuthis gahi*)**

**Andreas Winter**

**Natural Resources**

**Fisheries**

**June 2017**



## Index

Summary .....	2
Introduction.....	2
Methods.....	4
Stock assessment.....	8
Data.....	8
Group arrivals / depletion criteria.....	9
Depletion analyses .....	11
South.....	11
North.....	13
Escapement biomass.....	14
Immigration .....	16
Bycatch .....	16
References.....	19
Appendix.....	22
Falkland calamari individual weights.....	22
Prior estimates and CV .....	23
Depletion model estimates and CV .....	25
Combined Bayesian models .....	27
Natural mortality.....	28
Total catch by species.....	30

## Summary

- 1) The 2017 first season Falkland calamari fishery (C license) was open from February 27<sup>th</sup>, and closed by directed order on May 1<sup>st</sup>. Season start and close had been postponed by 3 days to allow participation in 30<sup>th</sup> anniversary events. Compensatory days for mechanical failures and bad weather resulted in 10 vessel-days taken after May 1<sup>st</sup>, with one vessel fishing as late as May 5<sup>th</sup>.
- 2) 39,433 tonnes of calamari catch were reported in the C-license fishery; the highest 1<sup>st</sup> season catch since 1995 and giving an average CPUE of 39.6 t vessel-day<sup>-1</sup>. Throughout the season 49.24% of calamari catch and 49.25% of fishing effort were taken north of 52° S; 50.76% of calamari catch and 50.75% of fishing effort were taken south of 52° S.
- 3) Sub-areas north and south of 52°S were depletion-modelled separately. In the north sub-area, two depletion periods / immigrations were inferred to have started on March 8<sup>th</sup> and March 28<sup>th</sup>. In the south sub-area, three depletion periods / immigrations were inferred to have started on February 27<sup>th</sup> (start of the season), April 20<sup>th</sup>, and May 1<sup>st</sup> – the last scheduled day of the season.
- 4) Approximately 65,154 tonnes of calamari (95% confidence interval: [51,729 to 214,193] tonnes) were estimated to have immigrated into the Loligo Box during first season 2017, of which 42,022 t north of 52° S and 23,131 t south of 52° S.
- 5) The escapement biomass estimate for calamari remaining in the Loligo Box at the end of first season 2017 was:  
Maximum likelihood of 45,655 tonnes, with a 95% confidence interval of [35,317 to 185,827] tonnes.  
The risk of calamari escapement biomass at the end of the season being less than 10,000 tonnes was estimated at effectively zero.

## Introduction

The first season of the 2017 Falkland calamari fishery (*Doryteuthis gahi* – Patagonian longfin squid – colloquially *Loligo*) opened on February 27<sup>th</sup>. Season opening was postponed 3 days past the end of the survey on February 23<sup>rd</sup> (Winter et al. 2017) by agreement between the FIG and Loligo Producers' Group, to give vessels the opportunity to participate in activities of the Falklands fishing industry 30<sup>th</sup> Anniversary. Fifteen C-licensed trawlers started the season on February 27<sup>th</sup>, with one trawler delayed by a day as it entered as a short-notice replacement for a different vessel that had experienced mechanical breakdown. During the season, another vessel was replaced for mechanical problems, and the replacement vessel inherited 3 breakdown flex days. Four vessels took one bad-weather day each (Figure 1). Two vessels performed one day each of experimental nearshore fishing for juvenile toothfish (*Dissostichus eleginoides*), and were allocated a compensatory additional C-license day. The season ended by directed closure on May 1<sup>st</sup>. The various schedule adjustments amounted to ten vessel-days being taken after May 1<sup>st</sup>, with the last vessel finishing on May 5<sup>th</sup>.

Total reported Falkland calamari catch under first season C license was 39,433 tonnes (Table 1), corresponding to an average CPUE of  $39433 / 997 = 39.6$  tonnes vessel-day<sup>-1</sup>. This average CPUE was the third-highest in a first season, following 2012 (45.2 t v-day<sup>-1</sup>) and 2005 (42.7 t v-day<sup>-1</sup>).

The Falkland calamari stock assessment was conducted with depletion time-series models as in previous seasons (Agnew et al. 1998, Roa-Ureta and Arkhipkin 2007; Arkhipkin et al. 2008), and other squid fisheries (Royer et al. 2002, Young et al. 2004, Chen et al. 2008, Morales-Bojórquez et al. 2008, Keller et al. 2015). Because calamari has an annual life cycle

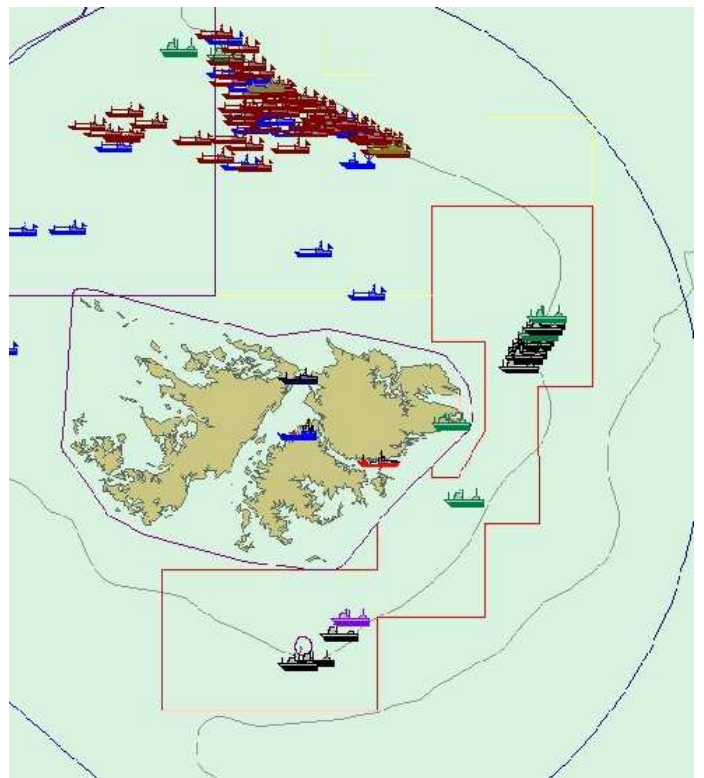
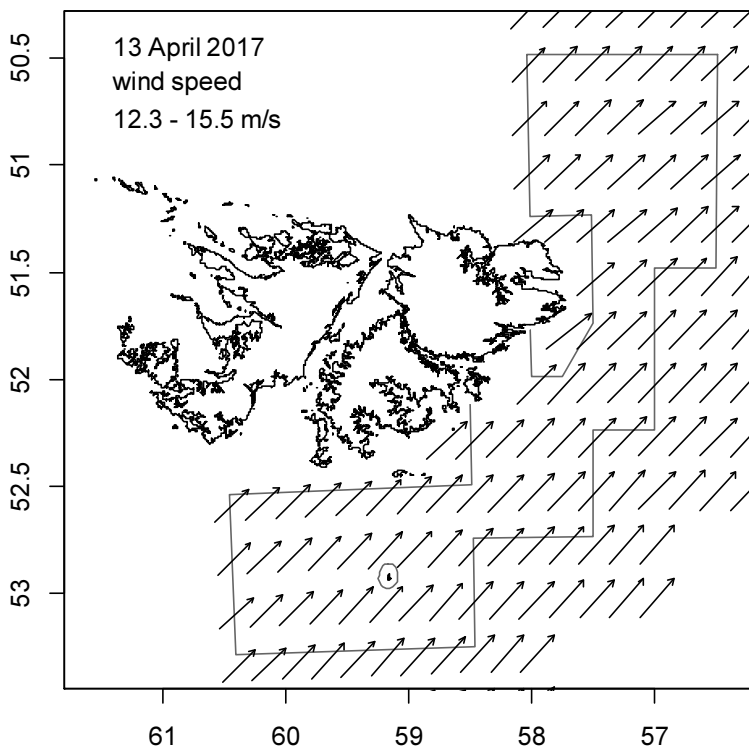
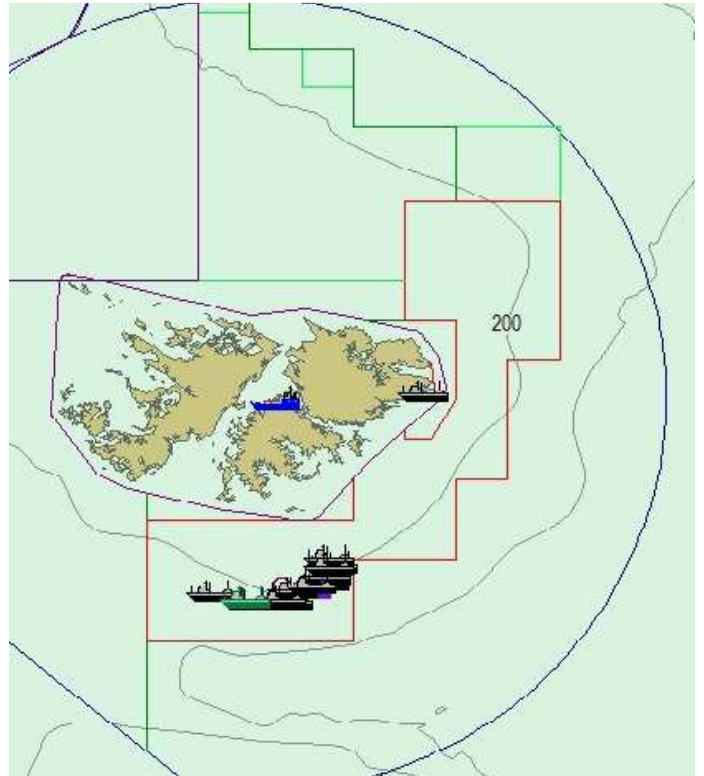
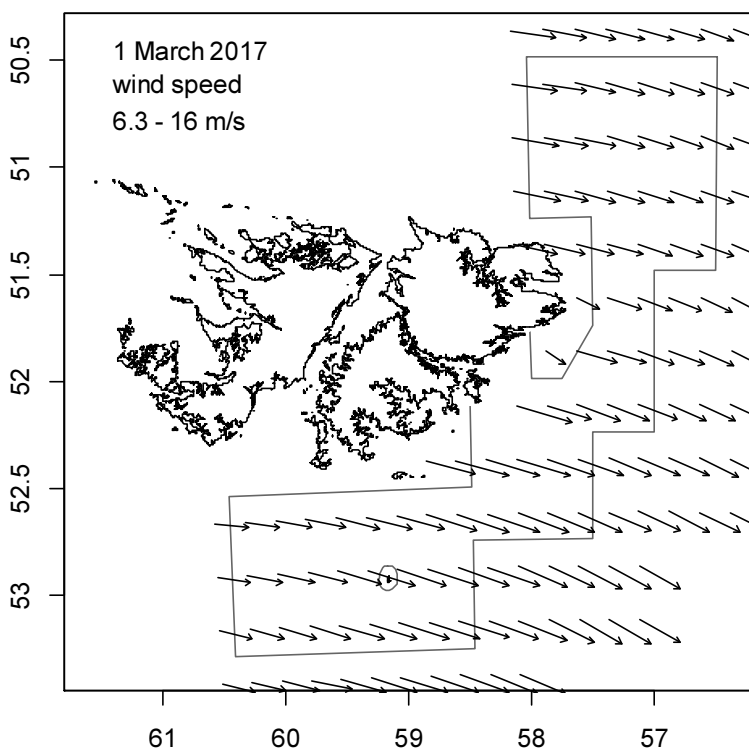


Figure 1. Left: wind speed vector plot at  $0.25^\circ$  resolution, from blended satellite observations (Zhang et al., 2006). Right: Fish Ops chart display. Top: March 1<sup>st</sup>, when 3 vessels declared bad-weather days, bottom: April 13<sup>th</sup>, when 1 vessel declared a bad-weather day.

(Patterson 1988), stock cannot be derived from a standing biomass carried over from prior years (Rosenberg et al. 1990, Pierce and Guerra 1994). The depletion model instead calculates an estimate of population abundance over time by evaluating what levels of abundance and catchability must be extant to sustain the observed rate of catch. Depletion modelling of the Falkland calamari fishery is used both in-season and for the post-season summary, with the objective of maintaining an escapement biomass of 10,000 tonnes calamari at the end of each season as a conservation threshold (Agnew et al. 2002, Barton 2002).

Table 1. Falkland calamari season comparisons since 2004, when catch management was assumed by the FIFD. Days: total number of calendar days open to licensed calamari fishing including (since 1<sup>st</sup> season 2013) optional extension days; V-Days: aggregate number of licensed calamari fishing days reported by all vessels for the season.

	Season 1			Season 2		
	Catch (t)	Days	V-Days	Catch (t)	Days	V-Days
2004	7,152	46	625	17,559	78	1271
2005	24,605	45	576	29,659	78	1210
2006	19,056	50	704	23,238	53	883
2007	17,229	50	680	24,171	63	1063
2008	24,752	51	780	26,996	78	1189
2009	12,764	50	773	17,836	59	923
2010	28,754	50	765	36,993	78	1169
2011	15,271	50	771	18,725	70	1099
2012	34,767	51	770	35,026	78	1095
2013	19,908	53	782	19,614	78	1195
2014	28,119	59	872	19,630	71	1099
2015	19,383*	57*	871*	10,190	42	665
2016	22,616	68	1020	23,089	68	1004
2017	39,433	68	999†			

\* Does not include C-license catch or effort after the C-license target for that season was switched from calamari to *Illex*.

† Includes two vessel-days of experimental fishing for juvenile toothfish.

## Methods

The depletion model formulated for the Falkland calamari stock is based on the equivalence:

$$C_{\text{day}} = q \times E_{\text{day}} \times N_{\text{day}} \times e^{-M/2} \quad (1)$$

where  $q$  is the catchability coefficient,  $M$  is the natural mortality rate (considered constant at  $0.0133 \text{ day}^{-1}$ ; Roa-Ureta and Arkhipkin 2007), and  $C_{\text{day}}$ ,  $E_{\text{day}}$ ,  $N_{\text{day}}$  are catch (numbers of calamari), fishing effort (numbers of vessels), and abundance (numbers of calamari) per day. In its basic form (DeLury 1947) the depletion model assumes a closed population in a fixed area for the duration of the assessment. However, the assumption of a closed population is imperfectly met in the Falkland Islands fishery, where stock analyses have often shown that calamari groups arrive in successive waves after the start of the season (Roa-Ureta 2012; Winter and Arkhipkin 2015). Arrivals of successive groups are inferred from discontinuities in the catch data. Fishing on a single, closed cohort would be expected to yield gradually

decreasing CPUE, but gradually increasing average individual sizes, as the squid grow. When instead these data change suddenly, or in contrast to expectation, the immigration of a new group to the population is indicated (Winter and Arkhipkin 2015).

In the event of a new group arrival, the depletion calculation must be modified to account for this influx. This was done using a simultaneous algorithm (Roa-Ureta 2012) that adds new arrivals on top of the stock previously present, and posits a common catchability coefficient for the entire depletion time-series. If two depletions are included in the same model (i.e., the stock present from the start plus a new group arrival), then:

$$C_{\text{day}} = q \times E_{\text{day}} \times (N1_{\text{day}} + (N2_{\text{day}} \times i2_{|_0}^1)) \times e^{-M/2} \quad (2)$$

where  $i2$  is a dummy variable taking the values 0 or 1 if ‘day’ is before or after the start day of the second depletion. For more than two depletions,  $N3_{\text{day}}$ ,  $i3$ ,  $N4_{\text{day}}$ ,  $i4$ , etc., would be included following the same pattern.

The Falkland calamari stock assessment was calculated in a Bayesian framework (Punt and Hilborn, 1997), whereby results of the season depletion model are conditioned by prior information on the stock; in this case the information from the pre-season survey. The season depletion likelihood function was calculated as the difference between actual catch numbers reported and catch numbers predicted from the model (Equation 2), statistically corrected by a factor relating to the number of days of the depletion period (Roa-Ureta, 2012):

$$((n\text{Days} - 2) / 2) \times \log \left( \sum_{\text{days}} \left( \log(\text{predicted } C_{\text{day}}) - \log(\text{actual } C_{\text{day}}) \right)^2 \right) \quad (3)$$

The prior likelihood function was calculated as the normal distribution of the difference between catchability ( $q$ ) derived from the survey abundance estimate, and catchability derived from the season depletion model:

$$\frac{1}{\sqrt{2\pi \cdot SD_{q \text{ prior}}^2}} \times \exp \left( -\frac{(q_{\text{model}} - q_{\text{prior}})^2}{2 \cdot SD_{q \text{ prior}}^2} \right) \quad (4)$$

where the standard deviation of catchability ( $q$ ) prior is calculated from the Euclidean sum of the survey prior estimate uncertainty, the variability in catches on the season start date, and the uncertainty in the natural mortality  $M$  estimate over the number of days mortality discounting (Equation A5-S). Catchability, rather than abundance  $N$ , was used for calculating the prior likelihood because catchability informs the entire season time series; whereas  $N$  from the survey only informs the first season depletion period – subsequent immigrations and depletions are independent of the abundance that was present during the survey.

Bayesian optimization of the depletion was calculated by jointly minimizing Equations 3 and 4, using the Nelder-Mead algorithm in R programming package ‘optimx’ (Nash and Varadhan, 2011). Relative weights in the joint optimization were assigned to Equations 3 and 4 as the converse of their coefficients of variation (CV), i.e., the CV of the prior became the weight of the depletion model and the CV of the depletion model became the weight of the prior. Calculations of the CVs are described in the Appendix. Because a complex model with multiple depletions may converge on a local rather than global minimum, the optimization was stabilized by running a feed-back loop that set the  $q$  and  $N$

parameter outputs of the Bayesian joint optimization back into the in-season only minimization (Equation 3), re-calculated this minimization and the CV resulting from it, then re-calculated the Bayesian joint optimization, and continued this process until both the in-season minimization and the joint optimization remained unchanged.

With  $C_{\text{day}}$ ,  $E_{\text{day}}$  and  $M$  being fixed parameters, the optimization of Equation 2 using 3 and 4 produces estimates of  $q$  and  $N_1, N_2, \dots$ , etc. Numbers of calamari on the final day (or any other day) of a time series are then calculated as the numbers  $N$  of the depletion start days discounted for natural mortality during the intervening period, and subtracting cumulative catch also discounted for natural mortality (CNMD). Taking for example a two-depletion period:

$$N_{\text{final day}} = N_1_{\text{start day 1}} \times e^{-M(\text{final day} - \text{start day 1})} + N_2_{\text{start day 2}} \times e^{-M(\text{final day} - \text{start day 2})} - \text{CNMD}_{\text{final day}} \quad (5)$$

where

$$\text{CNMD}_{\text{day 1}} = 0$$

$$\text{CNMD}_{\text{day x}} = \text{CNMD}_{\text{day x-1}} \times e^{-M} + C_{\text{day x-1}} \times e^{-M/2} \quad (6)$$

$N_{\text{final day}}$  is then multiplied by the average individual weight of calamari on the final day to give biomass. Daily average individual weight is obtained from length / weight conversion of mantle lengths measured in-season by observers, and also derived from in-season commercial data as the proportion of product weight that vessels reported per market size category. Observer mantle lengths are scientifically accurate, but restricted to 1-2 vessels at any one time that may or may not be representative of the entire fleet, and not available every day. Commercially proportioned mantle lengths are relatively less accurate, but cover the entire fishing fleet every day. Therefore, both sources of data are used (see Appendix).

Distributions of the likelihood estimates from joint optimization (i.e., measures of their statistical uncertainty) were computed using a Markov Chain Monte Carlo (MCMC) (Gelman and Lopes 2006), a method that is commonly employed for fisheries assessments (Magnusson et al. 2013). MCMC is an iterative process which generates random stepwise changes to the proposed outcome of a model (in this case, the  $q$  and  $N$  of calamari) and at each step, accepts or nullifies the change with a probability equivalent to how well the change fits the model parameters compared to the previous step. The resulting sequence of accepted or nullified changes (i.e., the ‘chain’) approximates the likelihood distribution of the model outcome. The MCMC of the depletion models were run for 200,000 iterations; the first 1000 iterations were discarded as burn-in sections (initial phases over which the algorithm stabilizes); and the chains were thinned by a factor equivalent to the maximum of either 5 or the inverse of the acceptance rate (e.g., if the acceptance rate was 12.5%, then every 8<sup>th</sup> ( $0.125^{-1}$ ) iteration was retained) to reduce serial correlation. For each model three chains were run; one chain initiated with the parameter values obtained from the joint optimization of Equations 3 and 4, one chain initiated with these parameters  $\times 2$ , and one chain initiated with these parameters  $\times 1/4$ . Convergence of the three chains was accepted if the variance among chains was less than 10% higher than the variance within chains (Brooks and Gelman 1998). When convergence was satisfied the three chains were combined as one final set. Equations 5, 6, and the multiplication by average individual weight were applied to the CNMD and each iteration of  $N$  values in the final set, and the biomass outcomes from these calculations

represent the distribution of the estimate. The peaks of the MCMC histograms were compared to the empirical optimizations of the N values.

Total escapement biomass is defined as the aggregate biomass of calamari on the last day of the season for north and south sub-areas combined. Calamari sub-stocks emigrate from different spawning grounds and remain to an extent segregated (Arkhipkin and Middleton 2002). However, it is not assumed that north and south biomasses are uncorrelated (Shaw et al. 2004), and therefore north and south likelihood distributions were added semi-randomly in proportion to the strength of their day-to-day correlation (see Winter 2014, for the semi-randomization algorithm).

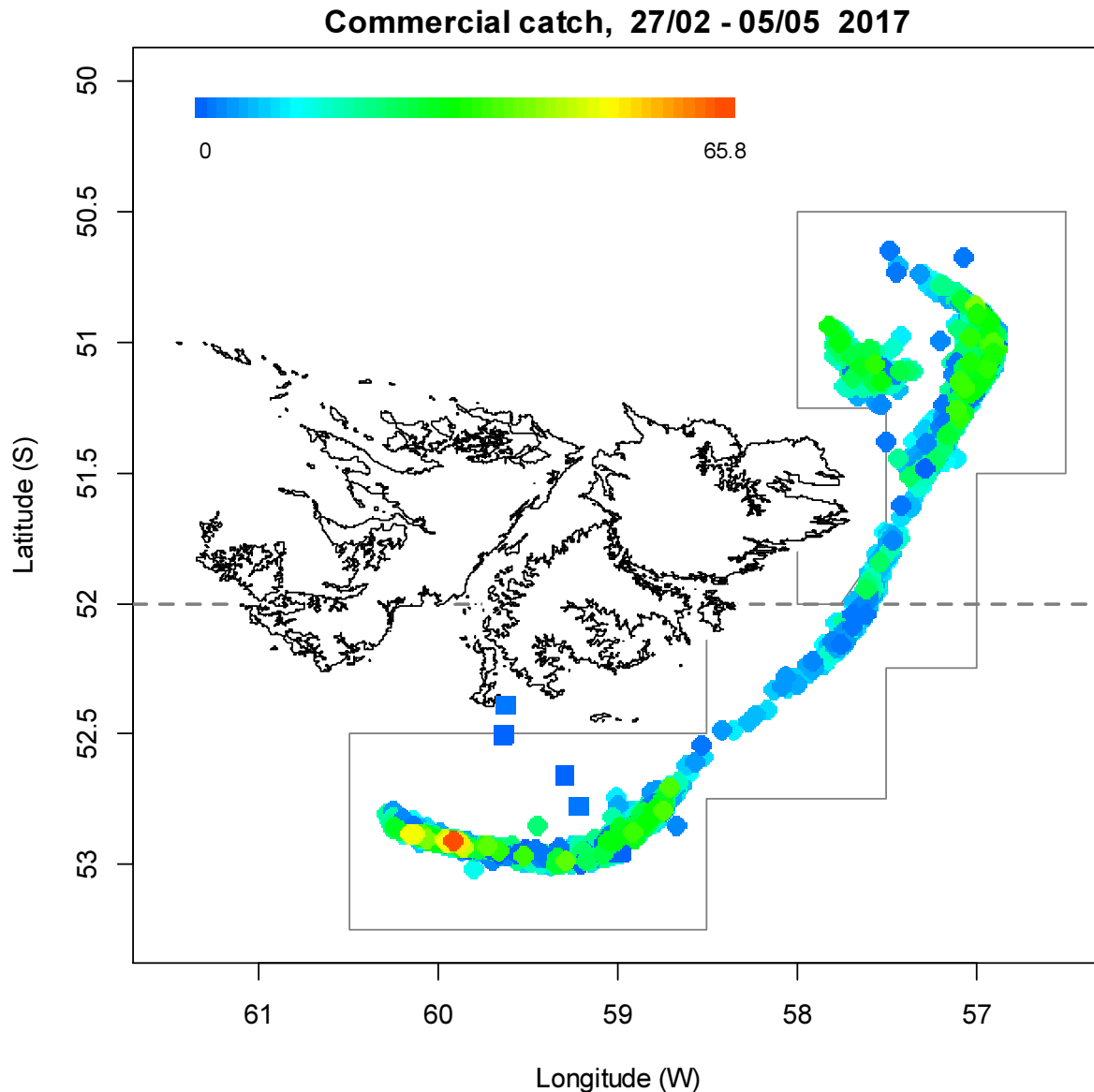


Figure 2. Spatial distribution of Falkland calamari 1<sup>st</sup>-season trawls, colour-scaled to catch weight (max. = 65.8 tonnes). 2961 trawl catches were taken during the season. Trawls taken for juvenile toothfish experimental fishing are shown as squares. These toothfish trawls were under E licence, but are included as de facto in-season catches. The ‘Loligo Box’ fishing zone, as well as the 52 °S parallel delineating the boundary between north and south assessment sub-areas, are shown in grey.

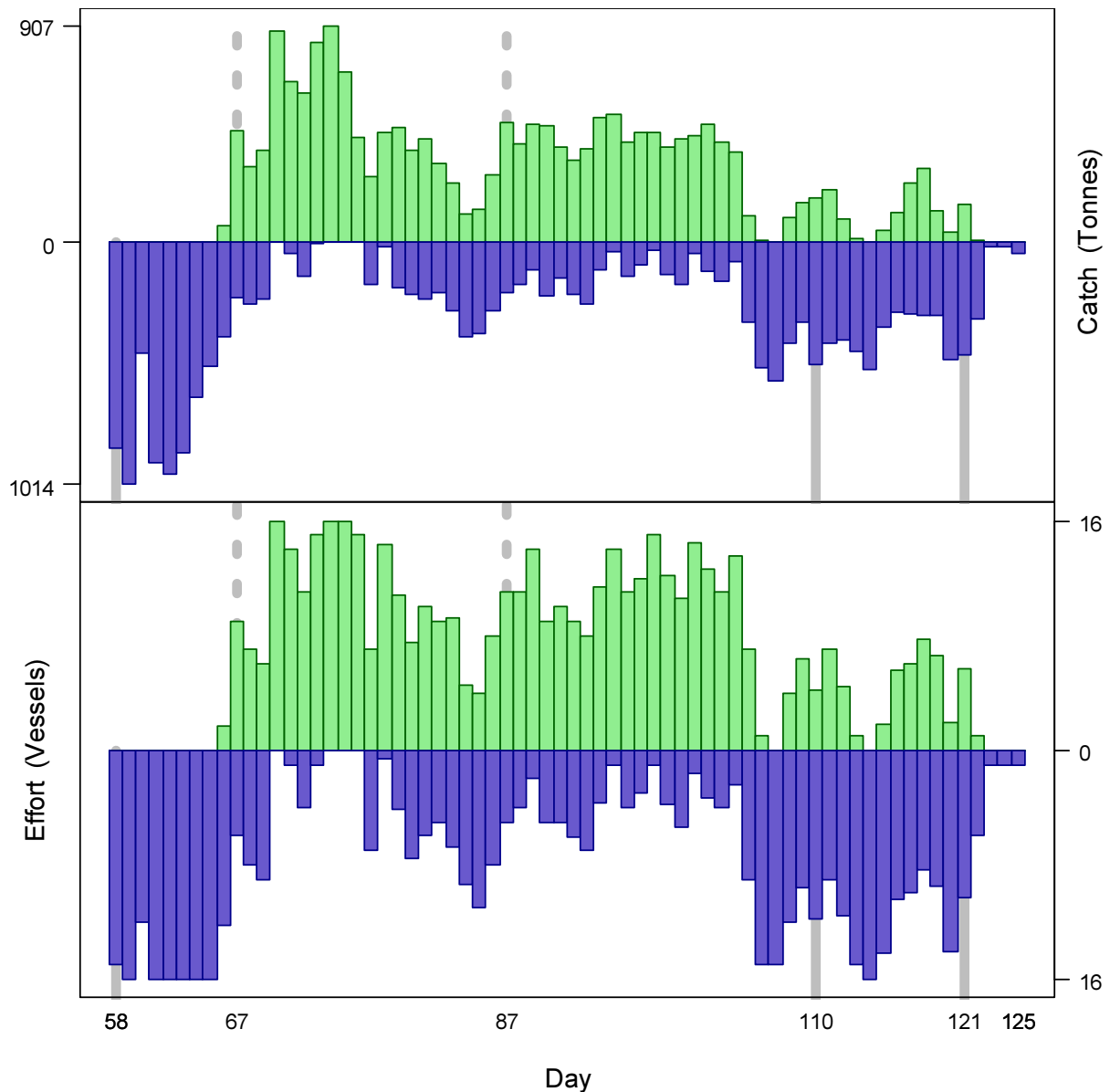


Figure 3. Daily total Falkland calamari catch and effort distribution by assessment sub-area north (green) and south (purple) of the 52° S parallel during 1<sup>st</sup> season 2017. The season was open from February 27<sup>th</sup> (chronological day 58) to May 1<sup>st</sup> (chronological day 121), plus flex days until May 5<sup>th</sup> (day 125). As many as 16 vessels fished per day north of 52° S; as many as 16 vessels fished per day south of 52° S. As much as 907 tonnes calamari was caught per day north of 52° S; as much as 1014 tonnes calamari was caught per day south of 52° S.

## Stock assessment

### Data

Total fishing effort in the 1<sup>st</sup> season 2017 was distributed evenly and proportionally with 49.24% of calamari catch and 49.25% of effort in the north sub-area (north of 52° S); 50.76% of catch and 50.75% of effort in the south sub-area. Highest catches and effort were concentrated towards the extremities of both the north and south sub-areas (Figure 2). The fishery was concentrated in three main blocks of time: from the start of the season until March 7<sup>th</sup> (day 66) 1.3% of fishing effort was taken north and 98.7% south; between March

8<sup>th</sup> and April 15<sup>th</sup> (day 105) 71.4% of fishing effort was taken north and 28.6% south; and from April 16<sup>th</sup> to the end of the season 24.2% of fishing effort was taken north and 75.8% south (Figure 3).

A total of 999 vessel-days were fished during the season (Table 1), with a median of 16 vessels per day (mean 15.45) except for flex and weather extensions. Vessels reported daily catch totals to the FIFD and electronic logbook data that included trawl times, positions, and product weight by market size categories. Three FIFD observers were deployed on four vessels in the fishery for a total of 94 observer-days (Bradley 2017a; 2017b, Boag 2017, Iriarte 2017). Throughout the 68 days of the season, 4 days had no observer covering (3 of which were extension days), 34 days had 1 observer covering, and 30 days had two observers covering. The seabird observing protocol in the calamari fishery was modified this season so that observers spent a half day monitoring seabird-vessel interactions (shooting, trawling, hauling) every two days, alternating half-days between morning and afternoon. On those seabird days the fish observing quota was halved from working two trawls to one trawl. Throughout the season observers sampled an average of 386.2 calamari daily, and reported their maturity stages, sex, and lengths to 0.5 cm. The length-weight relationship for converting both observer and commercially proportioned length data was taken from the pre-season survey (Winter et al. 2017):

$$\text{weight (kg)} = 0.162 \times \text{length (cm)}^{2.253} / 1000 \quad (7)$$

### Group arrivals / depletion criteria

Start days of depletions - following arrivals of new calamari groups - were judged primarily by daily changes in CPUE, with additional information from sex proportions, maturity, and average individual calamari sizes. CPUE was calculated as metric tonnes of calamari caught per vessel per day. Days were used rather than trawl hours as the basic unit of effort. Commercial vessels do not trawl standardized duration hours, but rather durations that best suit their daily processing requirements. An effort index of days is therefore more consistent.

Three days in the south and two days in the north were identified that represented the onset of separate immigrations / depletions in the season.

- The first depletion south was identified on day 58 (February 27<sup>th</sup> – start of the commercial season) with 15 vessels starting the fishery in the south (Figure 3) and low average maturities (Figure 4D). CPUE was 57.4 t vessel<sup>-1</sup> day<sup>-1</sup>, increasing to 63.4 t vessel<sup>-1</sup> day<sup>-1</sup> the next day; highest of the season.
- The second depletion south was identified on day 110 (April 20<sup>th</sup>) with a resurgence of CPUE (Figure 5), and commercial weight averages, observer weight averages, and observer maturity averages that had all been at local minima the day before (Figure 4A, B and D). The proportion of females was the lowest of 7 consecutive days (Figure 4C).
- The third depletion south was identified on day 121 (May 1<sup>st</sup> – the official end of the season) with another increase in CPUE (Figure 5), and local minima of observer weight averages, female proportion, and observer maturity averages (Figure 4B, C, D).
- The first depletion north was identified on day 67 (March 8<sup>th</sup>), the first day that more than two vessels fished in the north sub-area. Observer weight averages continued an increasing trend for four subsequent days (Figure 4B).
- The second depletion north was identified on day 87 (March 28<sup>th</sup>) with an increase in CPUE (Figure 5) and one day after local minima in observer weight averages and maturity averages (Figure 4B and D).

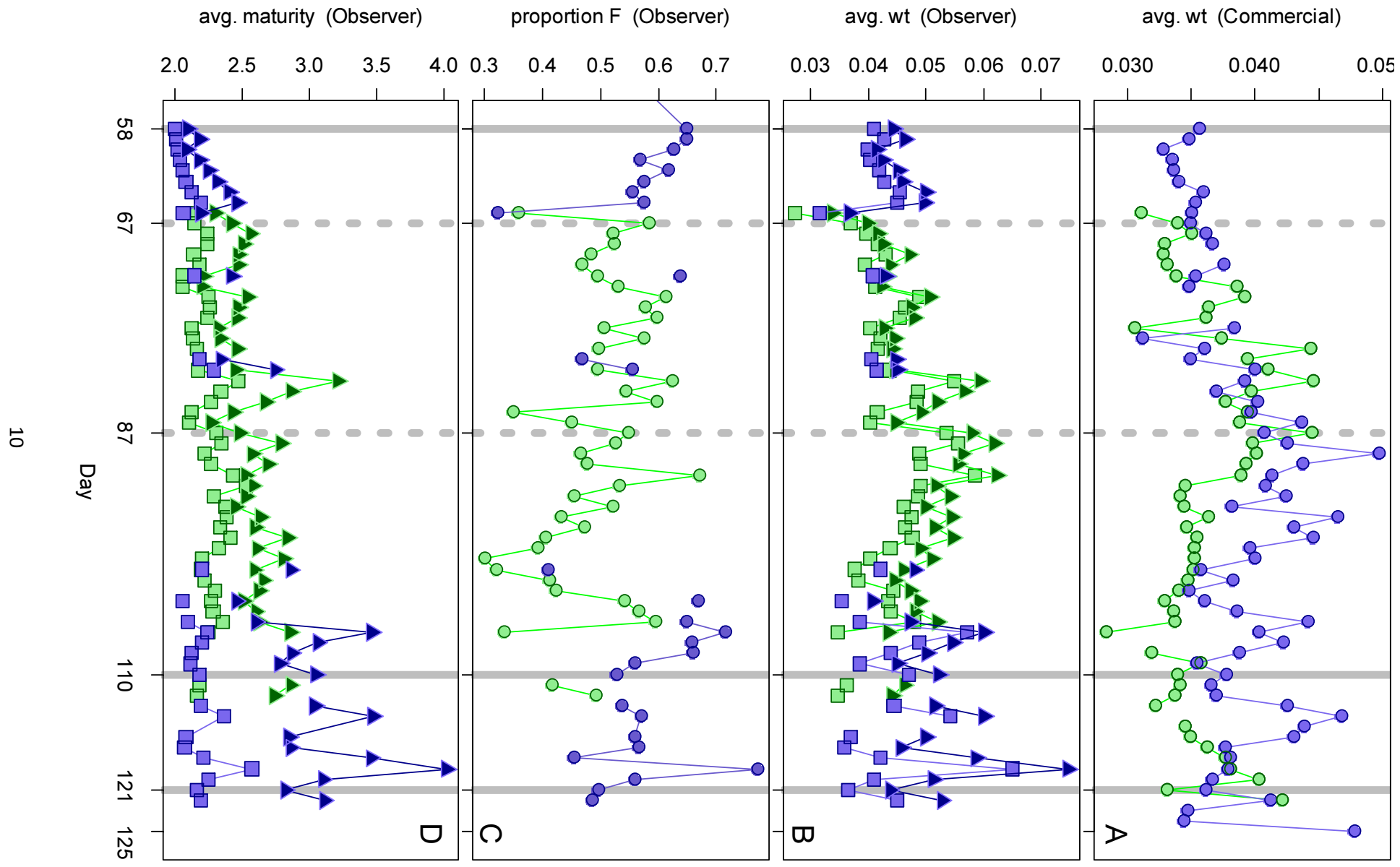


Figure 4 [previous page]. A: Average individual calamari weights (kg) per day from commercial size categories. B: Average individual calamari weights (kg) by sex per day from observer sampling. C: Proportions of female calamari per day from observer sampling. D: Average maturity value by sex per day from observer sampling. In all graphs – Males: triangles, females: squares, unsexed: circles. North sub-area: green, south sub-area: purple. Data from consecutive days are joined by line segments. Broken grey bars indicate the starts of in-season depletions north. Solid grey bars indicate the starts of in-season depletions south.

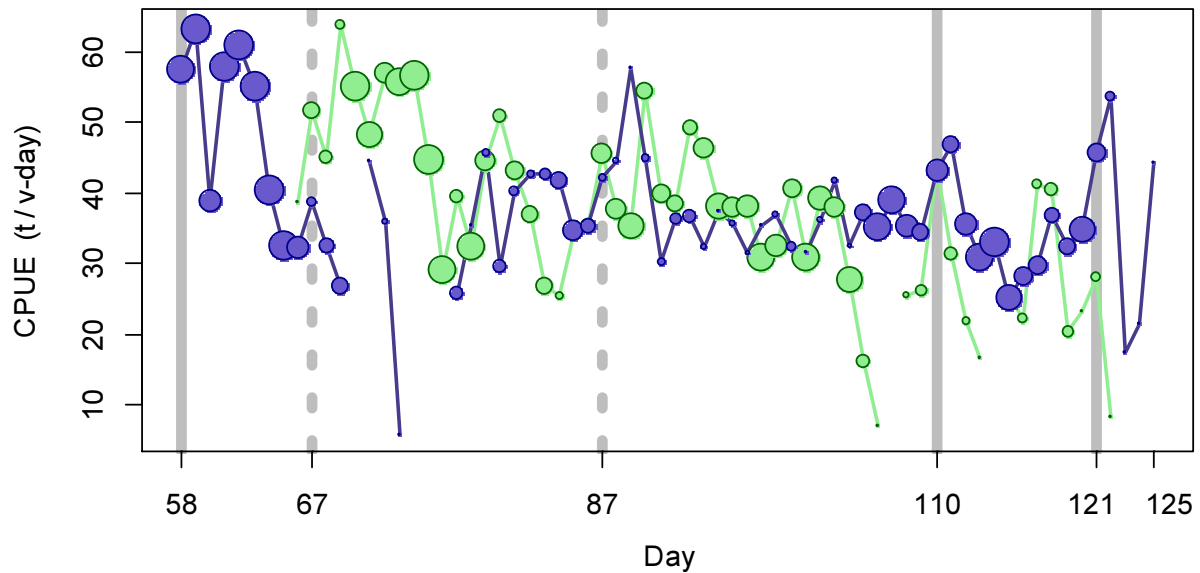


Figure 5. CPUE in metric tonnes per vessel per day, by assessment sub-area north (green) and south (purple) of 52° S latitude. Circle sizes are proportioned to numbers of vessels fishing. Data from consecutive days are joined by line segments. Broken grey bars indicate the starts of in-season depletions north. Solid grey bars indicate the starts of in-season depletions south.

## Depletion analyses

### South

In the south sub-area, Bayesian optimization on catchability ( $q$ ) resulted in a posterior (maximum likelihood Bayesian  $q_S = 1.005 \times 10^{-3}$ ; Figure 6, left, and Equation A9-S) that was intermediate between the pre-season prior (prior  $q_S = 1.355 \times 10^{-3}$ ; Figure 6, left, and Equation A4-S) and the in-season depletion  $q_S = 2.620 \times 10^{-10}$  (Figure 6, left, and A6-S). Bayesian optimization was weighted as the converse of the CVs: 0.710 for in-season depletion (A5-S) vs. 0.288 for the prior (A8-S). Relative weight on the prior was predictably low through the additional uncertainty elicited by the postponement of season start after the survey. Notwithstanding, the posterior was strongly driven by the prior as the low actual rate of depletion, and especially the occurrence of an immigration / depletion just shortly before the end of the season (Figure 7), vested the in-season depletion calculation with little selectivity.

Figure 6 [below]. South sub-area. Left: Likelihood distributions for calamari catchability. Red line: prior model (pre-season survey data), blue line: in-season depletion model, grey bars: combined Bayesian model posterior. Right: Likelihood distribution (grey bars) of escapement biomass, from Bayesian posterior and average individual calamari weight at the end of the season. Blue lines: maximum likelihood and 95% confidence interval. Note correspondence to Figure 7.

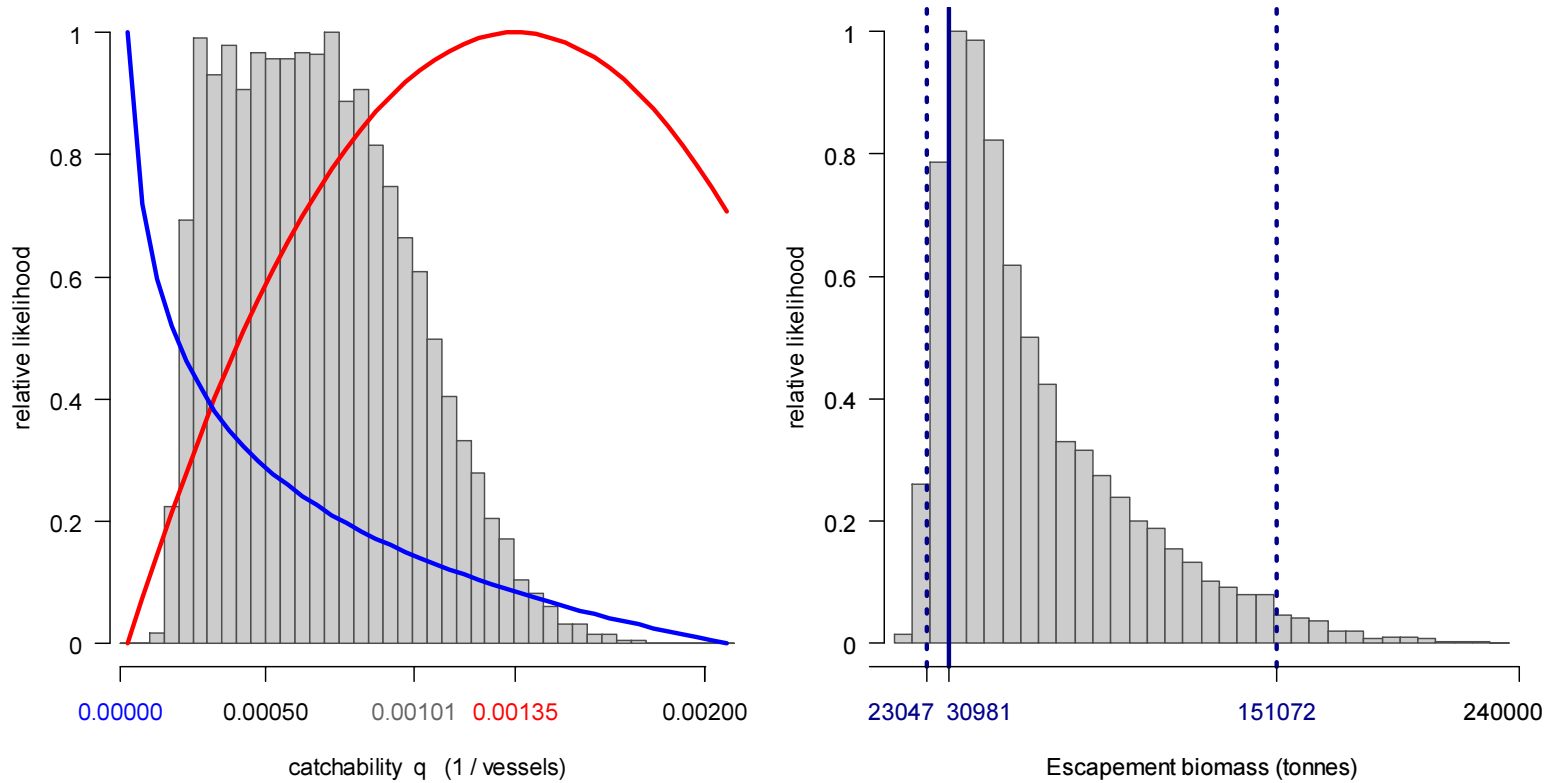
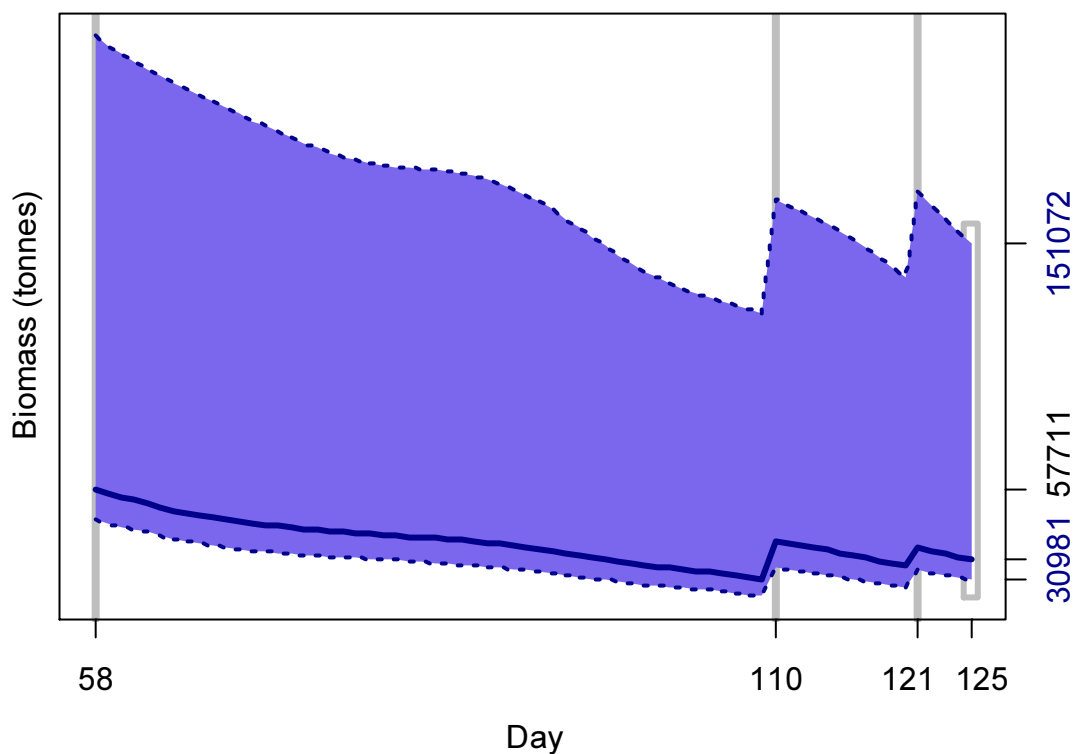


Figure 7 [below]. South sub-area. Calamari biomass time series estimated from Bayesian posterior of the depletion model  $\pm$  95% confidence intervals. Gray bars indicate the start of in-season depletions south; days 58, 110 and 121. Note that the biomass ‘footprint’ on day 125 (May 5<sup>th</sup>) corresponds to the right-side plot of Figure 6.



The MCMC distribution of the Bayesian posterior multiplied by the GAM fit of average individual calamari weight (Figure A1-south) gave the likelihood distribution of calamari biomass on day 125 (May 5<sup>th</sup>) shown in Figure 6-right, with maximum likelihood and 95% confidence interval of:

$$B_{S \text{ day } 125} = 30,981 \text{ t} \sim 95\% \text{ CI } [23,047 - 151,072] \text{ t} \quad (8)$$

At its highest point (on the first day of the season, day 58; February 27<sup>th</sup>), estimated calamari biomass south was 57,711 t  $\sim$  95% CI [46,188 – 230,319] t (Figure 7). Variability remained high throughout the time period, and it is not statistically conclusive that any change in average biomass occurred during the season by the rule (Swartzman et al. 1992) that a straight line could be drawn through the plot (Figure 7) without intersecting the 95% confidence intervals.

### North

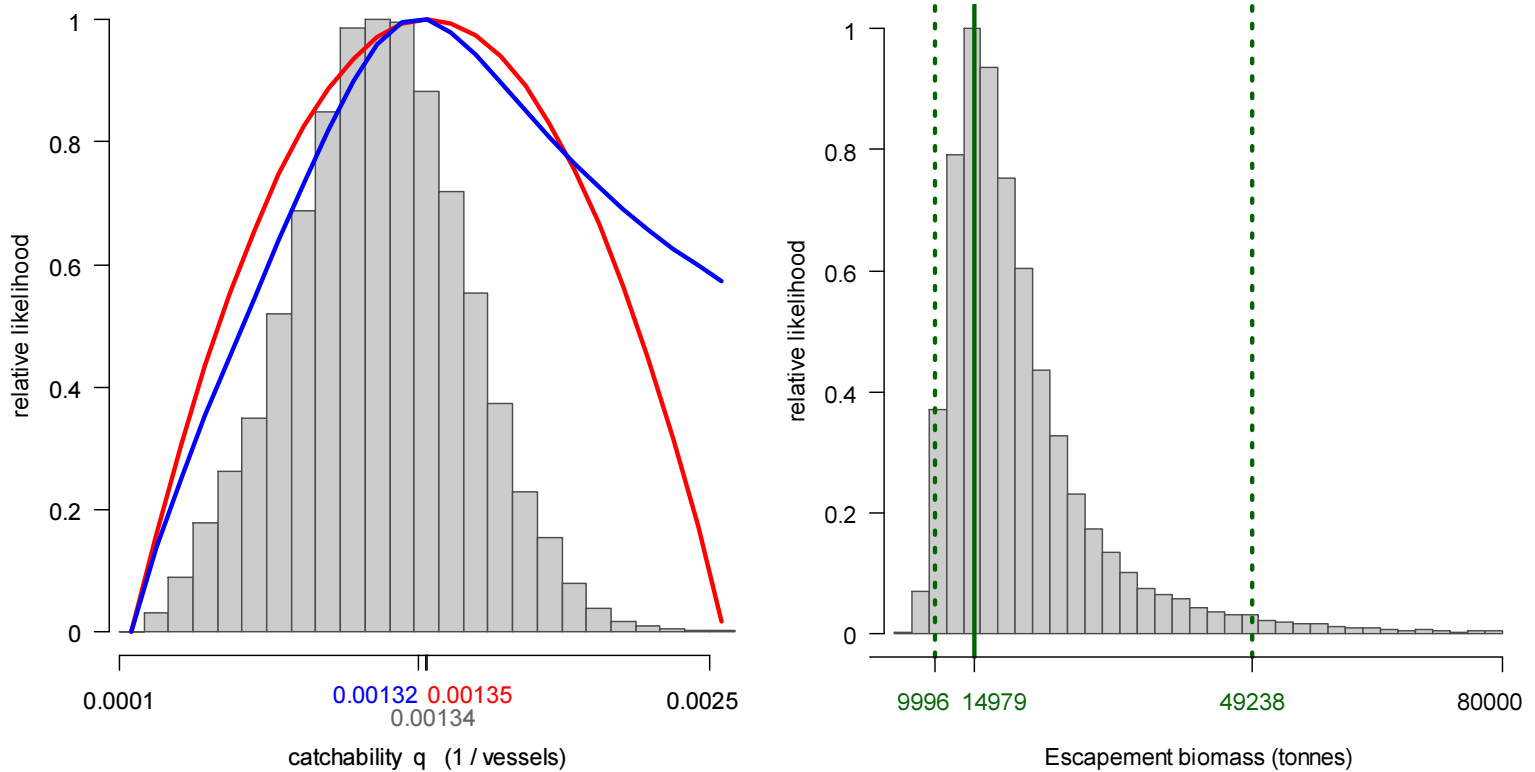
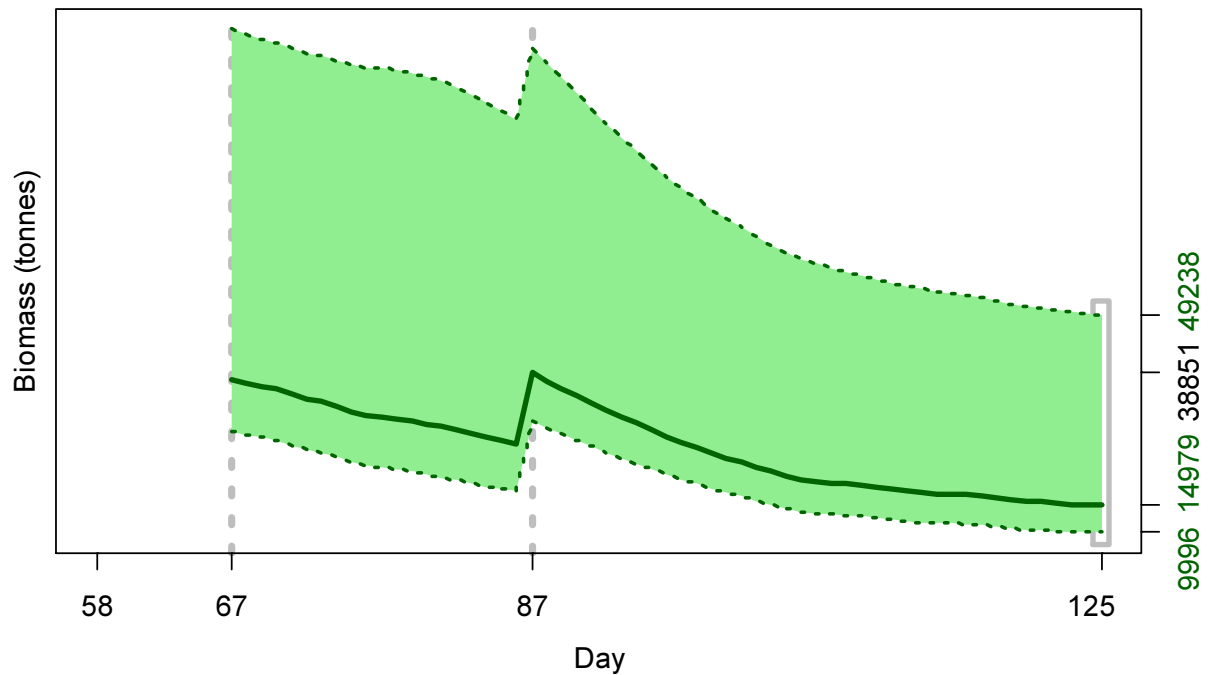


Figure 8. North sub-area. Left: Likelihood distributions for calamari catchability. Red line: prior model (pre-season survey data), blue line: in-season depletion model, grey bars: combined Bayesian model posterior. Right: Likelihood distribution (grey bars) of escapement biomass, from Bayesian posterior and average individual calamari weight at the end of the season. Green lines: maximum likelihood and 95% confidence interval. Note the correspondence to Figure 9.

Figure 9 [below]. North sub-area. Calamari biomass time series estimated from Bayesian posterior of the depletion model  $\pm$  95% confidence intervals. Broken grey bars indicate the start of in-season depletions north; days 67 and 87. Note that the biomass ‘footprint’ on day 125 (May 5<sup>th</sup>) corresponds to the right-side plot of Figure 8.



For the north sub-area, the Bayesian prior ( $\text{prior } q_N = 1.355 \times 10^{-3}$ ; Figure 8 left) was borrowed from the south as explained in the Appendix (A4-N). In-season depletion gave a very similar value at  $\text{depletion } q_N = 1.315 \times 10^{-3}$  (Figure 8 left, and Equation A6-N). The resulting Bayesian optimization on catchability ( $q$ ) (max. likelihood  $\text{Bayesian } q_N = 1.343 \times 10^{-3}$ ; Equation A9-N) was therefore close to both the prior and the in-season estimate (Figure 8, left). Respective weights in the Bayesian optimization were 0.710 for the in-season depletion (A5-N; again borrowed from the south) and 0.223 for the prior (A8-N).

The MCMC distribution of the Bayesian posterior multiplied by the GAM fit of average individual calamari weight (Figure A1-north) gave the likelihood distribution of calamari biomass on day 125 (May 5<sup>th</sup>) shown in Figure 8-right, with maximum likelihood and 95% confidence interval of:

$$B_{N \text{ day } 125} = 14,979 \text{ t} \sim 95\% \text{ CI } [9,996 - 49,238] \text{ t} \quad (9)$$

At its highest point (second depletion start: day 87 – March 28<sup>th</sup>), estimated calamari biomass north was 38,851 t  $\sim$  95% CI [30,282 – 97,762] t (Figure 9). Like the south biomass time series (Figure 7), the north biomass time series (Figure 9) did not show statistically significant change over the duration of the season.

### Escapement biomass

Total escapement biomass was defined as the aggregate biomass of Falkland calamari at the end of day 125 (May 5<sup>th</sup>) for north and south sub-areas combined (Equations 8 and 9). Depletion models are calculated on the inference that all fishing and natural mortality are gathered at mid-day, thus a half day of mortality ( $e^{-M/2}$ ) was added to correspond to the closure of the fishery at 23:59 (mid-night) on May 5<sup>th</sup> for the final remaining vessel: Equation 10. Semi-randomized addition of the north and south biomass estimates gave the aggregate likelihood distribution of total escapement biomass shown in Figure 10.

$$\begin{aligned}
B_{\text{Total day 125}} &= (B_{\text{N day 125}} + B_{\text{S day 125}}) \times e^{-M/2} \\
&= 45,960 \text{ t} \times 0.9934 \\
&= 45,655 \text{ t} \sim 95\% \text{ CI } [35,317 - 185,827] \text{ t}
\end{aligned}
\tag{10}$$

The risk of the fishery in the current season, defined as the proportion of the total escapement biomass distribution below the conservation limit of 10,000 tonnes (Agnew et al., 2002; Barton, 2002), was calculated as effectively zero.

The escapement biomass total of 45,655 tonnes was the highest in a 1<sup>st</sup> season since 2005 (Anon. 2005) and concurrently the season catch of 39,433 tonnes was the highest since 1995 (Payá 2010). Note that the escapement biomass of 45,655 is lower than the estimate of 48,559 tonnes given immediately after season end, as a data error in one vessel's catch size reporting has been corrected.

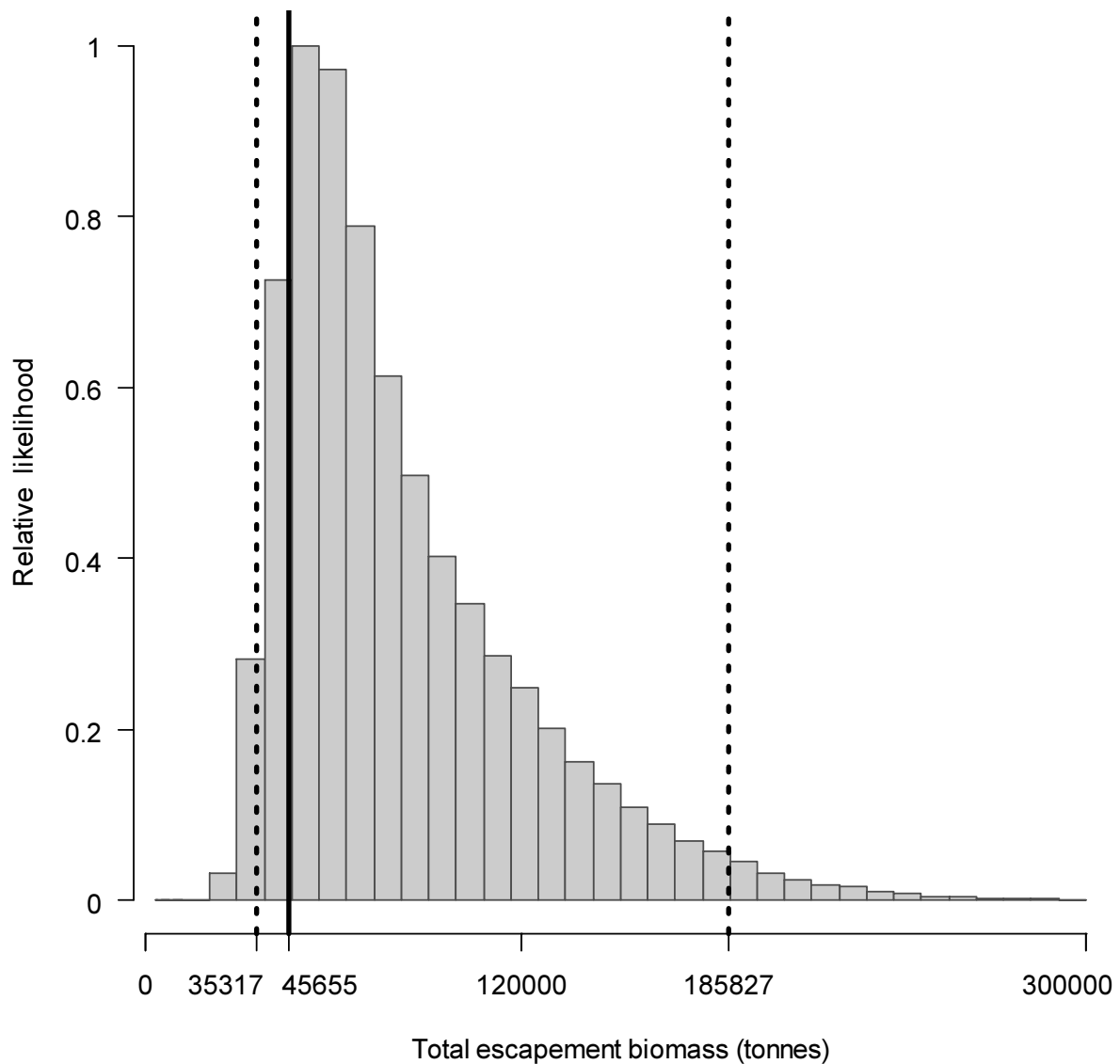


Figure 10. Likelihood distribution with 95% confidence intervals of total Falkland calamari escapement biomass corresponding to the season end (May 5<sup>th</sup>).

## Immigration

Falkland calamari immigration during the season was inferred on each day by how many more calamari were estimated present than the day before, minus the number caught and the number expected to have died naturally:

$$\text{Immigration } N_{\text{day } i} = N_{\text{day } i} - (N_{\text{day } i-1} - C_{\text{day } i-1} - M_{\text{day } i-1})$$

where  $N_{\text{day } i-1}$  are optimized in the depletion models,  $C_{\text{day } i-1}$  calculated as in Equation 2, and  $M_{\text{day } i-1}$  is:

$$M_{\text{day } i-1} = (N_{\text{day } i-1} - C_{\text{day } i-1}) \times (1 - e^{-M})$$

Immigration biomass per day was then calculated as the immigration number per day multiplied by predicted average individual weight from the GAM:

$$\text{Immigration } B_{\text{day } i} = \text{Immigration } N_{\text{day } i} \times \text{GAM } W_{t \text{ day } i}$$

All numbers  $N$  are themselves derived from the daily average individual weights, so the estimation factors in that those calamari immigrating on a day would likely be smaller than average. Confidence intervals of the immigration estimates were calculated by applying the above algorithms to the MCMC iterations of the depletion models. Resulting total biomasses of calamari immigration north and south, up to season end (day 125), were:

$$\text{Immigration } B_{N \text{ day } 67-125} = 42,022 \text{ t} \sim 95\% \text{ CI } [32,364 - 118,225] \text{ t} \quad \text{(11-N)}$$

$$\text{Immigration } B_{S \text{ day } 58-125} = 23,131 \text{ t} \sim 95\% \text{ CI } [16,288 - 118,142] \text{ t} \quad \text{(11-S)}$$

Total immigration with semi-randomized addition of the confidence intervals was:

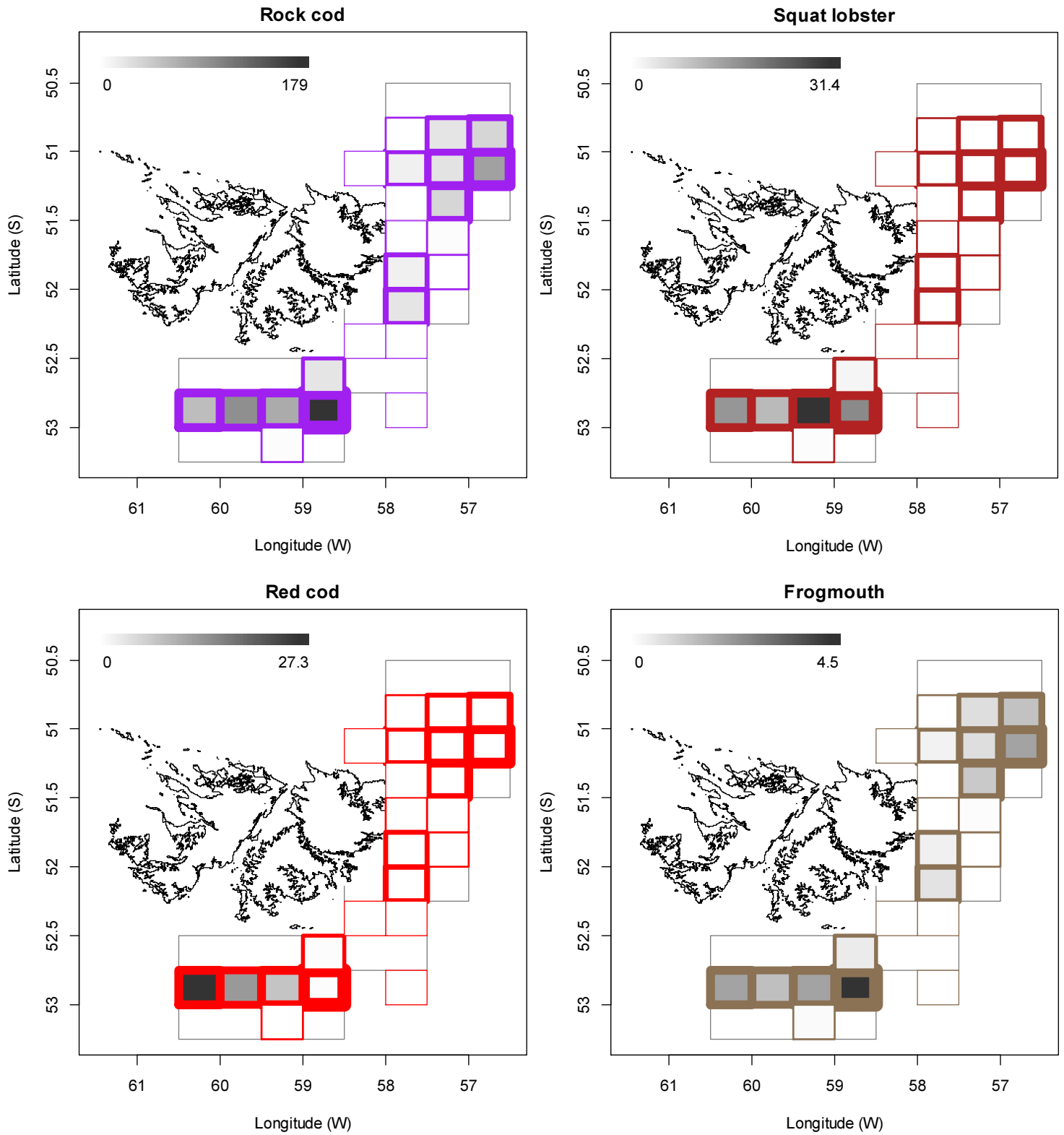
$$\text{Immigration } B_{\text{Total } 58-125} = 65,154 \text{ t} \sim 95\% \text{ CI } [51,729 - 214,193] \text{ t} \quad \text{(11-T)}$$

In the north sub-area, the in-season peak on day 87 accounted for approximately 30.3% of in-season immigration (Figure 9). Computationally, 67.4% was attributed to start day 67, but due to the time series gap after the end of the survey it is not determinate if immigration actually occurred on day 67. In the south sub-area, the in-season peaks on days 110 and 121 accounted for approximately 64.1% and 29.2% of in-season immigration (Figure 7).

## Bycatch

Of the 997 calamari-target 1<sup>st</sup> season vessel-days (Table 1), one single vessel-day reported a primary catch other than calamari: on April 26<sup>th</sup> 18.9 t red cod (*Salilota australis*) vs. 11.3 t calamari in grid XVAH. The most common total bycatches reported for the Falkland calamari season were rock cod (687 t, reported from 960 vessel-days), squat lobster (*Munida* spp.) (78 t, 171 vessel-days), red cod (50 t, 182 vessel-days), frogmouth (*Cottoperca gobio*) (18 t, 468 vessel-days), shortfin squid (*Illex argentinus*) (17 t, 267 vessel-days), common hake (*Merluccius hubbsi*) (10 t, 211 vessel-days), marbled rock cod (*Patagonotothen tessellata*) (9 t, 86 vessel-days), and Patagonian toothfish (*Dissostichus eleginoides*) (9 t, 161 vessel-days).

Relative distributions by grid of these bycatches are shown in Figure 11, and the complete list of all catches by species is given in Table A1.



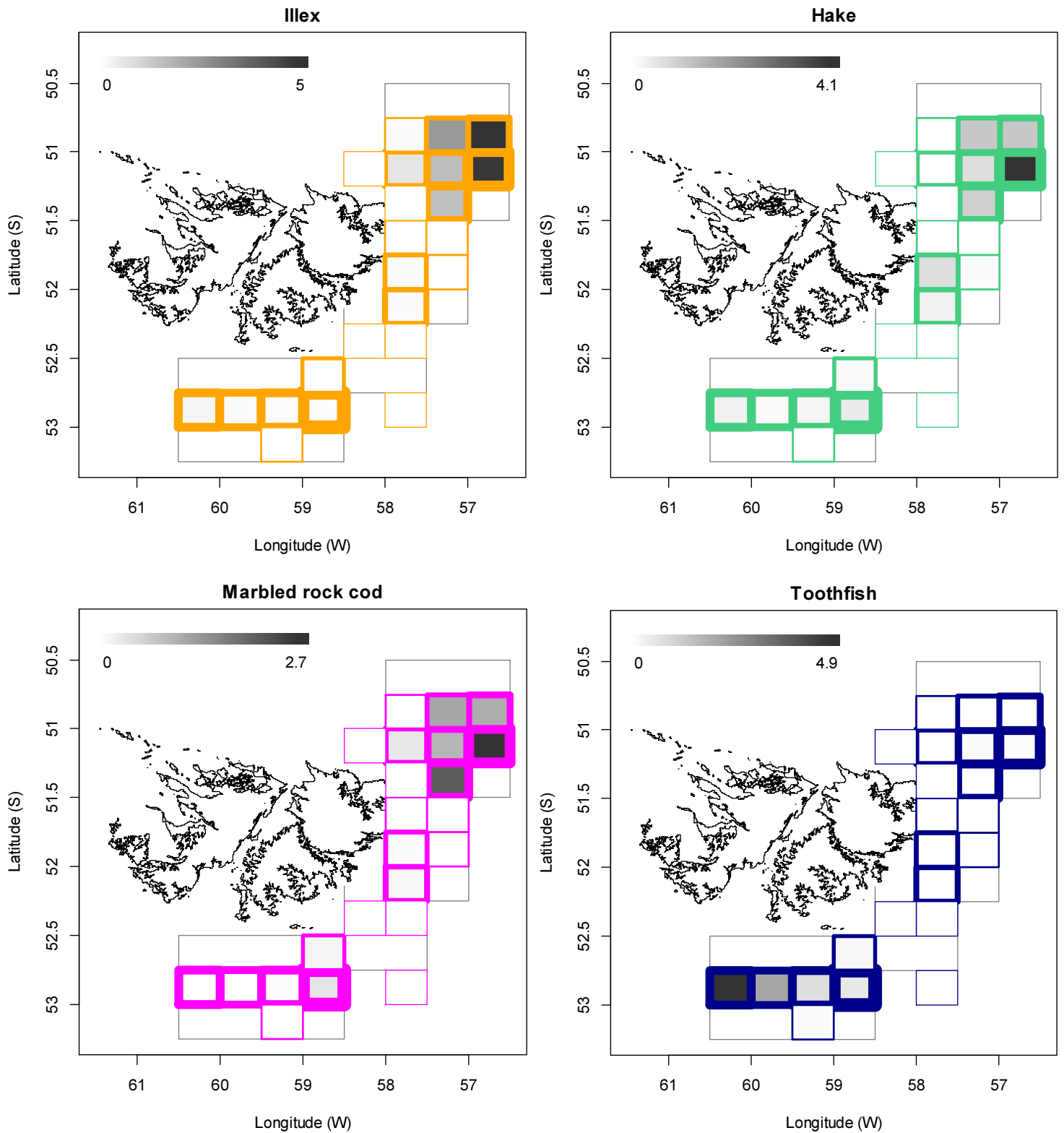


Figure 11. Distributions of the eight principal bycatches during 1<sup>st</sup> calamari season 2017, by noon position grids. Thickness of grid lines is proportional to the number of vessel-days (1 to 197 per grid; 23 different grids were occupied). Gray-scale is proportional to the bycatch biomass; maximum (tonnes) indicated on each plot.

## References

- Agnew, D.J., Baranowski, R., Beddington, J.R., des Clers, S., Nolan, C.P. 1998. Approaches to assessing stocks of *Loligo gahi* around the Falkland Islands. *Fisheries Research* 35: 155-169.
- Agnew, D. J., Beddington, J. R., and Hill, S. 2002. The potential use of environmental information to manage squid stocks. *Canadian Journal of Fisheries and Aquatic Sciences*, 59: 1851–1857.
- Anon. 2005. Fishery Report. *Loligo gahi*, First Season 2005. Fishery statistics, biological trends, stock assessment and risk analysis. Technical Document, Falkland Islands Fisheries Dept. 12 p.
- Arkhipkin, A.I., Middleton, D.A.J. 2002. Sexual segregation in ontogenetic migrations by the squid *Loligo gahi* around the Falkland Islands. *Bulletin of Marine Science* 71: 109-127.
- Arkhipkin, A.I., Middleton, D.A.J., Barton, J. 2008. Management and conservation of a short-lived fishery resource: *Loligo gahi* around the Falkland Islands. *American Fisheries Society Symposium* 49: 1243-1252.
- Barton, J. 2002. Fisheries and fisheries management in Falkland Islands Conservation Zones. *Aquatic Conservation: Marine and Freshwater Ecosystems* 12: 127–135.
- Boag, T. 2017. Observer Report 1133. Technical Document, FIG Fisheries Department. 36 p.
- Bradley, K. 2017a. Observer Report 1131. Technical Document, FIG Fisheries Department. 36 p.
- Bradley, K. 2017b. Observer Report 1138. Technical Document, FIG Fisheries Department. 33 p.
- Brooks, S.P., Gelman, A. 1998. General methods for monitoring convergence of iterative simulations. *Journal of computational and graphical statistics* 7:434-455.
- Chen, X., Chen, Y., Tian, S., Liu, B., Qian, W. 2008. An assessment of the west winter-spring cohort of neon flying squid (*Ommastrephes bartramii*) in the Northwest Pacific Ocean. *Fisheries Research* 92: 221-230.
- DeLury, D.B. 1947. On the estimation of biological populations. *Biometrics* 3: 145-167.
- Gamerman, D., Lopes, H.F. 2006. Markov Chain Monte Carlo. Stochastic simulation for Bayesian inference. 2nd edition. Chapman & Hall/CRC.
- Hoenig, J.M. 1983. Empirical use of longevity data to estimate mortality rates. *Fishery Bulletin* 82: 898-903.
- Iriarte, V. 2017. Observer Report 1129. Technical Document, FIG Fisheries Department. 21 p.
- Jiao, Y., Cortés, E., Andrews, K., Guo, F. 2011. Poor-data and data-poor species stock assessment using a Bayesian hierarchical approach. *Ecological Applications* 21: 2691-2708.
- Keller, S., Robin, J.P., Valls, M., Gras, M., Cabanellas-Reboredo, M., Quetglas, A. 2015. The use of depletion models to assess Mediterranean cephalopod stocks under the current EU data collection framework. *Mediterranean Marine Science* 16: 513-523.
- Magnusson, A., Punt, A., Hilborn, R. 2013. Measuring uncertainty in fisheries stock assessment: the delta method, bootstrap, and MCMC. *Fish and Fisheries* 14: 325-342.

- Morales-Bojórquez, E., Hernández-Herrera, A., Cisneros-Mata, M.A., Nevárez-Martínez, M.O. 2008. Improving estimates of recruitment and catchability of jumbo squid *Dosidicus gigas* in the Gulf of California, Mexico. *Journal of Shellfish Research* 27: 1233-1237.
- Nash, J.C., Varadhan, R. 2011. optimx: A replacement and extension of the optim() function. R package version 2011-2.27. <http://CRAN.R-project.org/package=optimx>
- Patterson, K.R. 1988. Life history of Patagonian squid *Loligo gahi* and growth parameter estimates using least-squares fits to linear and von Bertalanffy models. *Marine Ecology Progress Series* 47: 65-74.
- Payá, I. 2010. Fishery Report. *Loligo gahi*, Second Season 2009. Fishery statistics, biological trends, stock assessment and risk analysis. Technical Document, Falkland Islands Fisheries Dept. 54 p.
- Pierce, G.J., Guerra, A. 1994. Stock assessment methods used for cephalopod fisheries. *Fisheries Research* 21: 255 – 285.
- Punt, A.E., Hilborn, R. 1997. Fisheries stock assessment and decision analysis: the Bayesian approach. *Reviews in Fish Biology and Fisheries* 7:35-63.
- Roa-Ureta, R. 2012. Modelling in-season pulses of recruitment and hyperstability-hyperdepletion in the *Loligo gahi* fishery around the Falkland Islands with generalized depletion models. *ICES Journal of Marine Science* 69: 1403–1415.
- Roa-Ureta, R., Arkhipkin, A.I. 2007. Short-term stock assessment of *Loligo gahi* at the Falkland Islands: sequential use of stochastic biomass projection and stock depletion models. *ICES Journal of Marine Science* 64: 3-17.
- Rosenberg, A.A., Kirkwood, G.P., Crombie, J.A., Beddington, J.R. 1990. The assessment of stocks of annual squid species. *Fisheries Research* 8: 335-350.
- Royer, J., Périès, P., Robin, J.P. 2002. Stock assessments of English Channel loliginid squids: updated depletion methods and new analytical methods. *ICES Journal of Marine Science* 59: 445-457.
- Shaw, P.W., Arkhipkin, A.I., Adcock, G.J., Burnett, W.J., Carvalho, G.R., Scherbich, J.N., Villegas, P.A. 2004. DNA markers indicate that distinct spawning cohorts and aggregations of Patagonian squid, *Loligo gahi*, do not represent genetically discrete subpopulations. *Marine Biology*, 144: 961-970.
- Su, Z., Adkison, M.D., Van Alen, B.W. 2001. A hierarchical Bayesian model for estimating historical salmon escapement and escapement timing. *Canadian Journal of Fisheries and Aquatic Sciences* 58: 1648-1662.
- Swartzman, G., Huang, C., Kaluzny, S. 1992. Spatial analysis of Bering Sea groundfish survey data using generalized additive models. *Canadian Journal of Fisheries and Aquatic Sciences* 49: 1366-1378.
- Winter, A. 2014. *Loligo* stock assessment, second season 2014. Technical Document, Falkland Islands Fisheries Department. 30 p.
- Winter, A. 2015. *Loligo* stock assessment, first season 2015. Technical Document, Falkland Islands Fisheries Department. 28 p.
- Winter, A. 2016. Falkland calamari stock assessment, second season 2016. Technical Document, Falkland Islands Fisheries Department. 28 p.

- Winter, A., Arkhipkin, A. 2015. Environmental impacts on recruitment migrations of Patagonian longfin squid (*Doryteuthis gahi*) in the Falkland Islands with reference to stock assessment. Fisheries Research 172: 85-95.
- Winter, A., Jones, J., Shcherbich, Z., Iriarte, V. 2017. Falkland calamari stock assessment survey, 1<sup>st</sup> season 2017. Technical Document, Falkland Islands Fisheries Department. 17 p.
- Young, I.A.G., Pierce, G.J., Daly, H.I., Santos, M.B., Key, L.N., Bailey, N., Robin, J.-P., Bishop, A.J., Stowasser, G., Nyegaard, M., Cho, S.K., Rasero, M., Pereira, J.M.F. 2004. Application of depletion methods to estimate stock size in the squid *Loligo forbesi* in Scottish waters (UK). Fisheries Research 69: 211-227.
- Zhang, H.-M., Bates, J.J., Reynolds, R.W. 2006. Assessment of composite global sampling: Sea surface wind speed. Geophysical Research Letters 33: L17714.

**Appendix**  
**Falkland calamari individual weights**

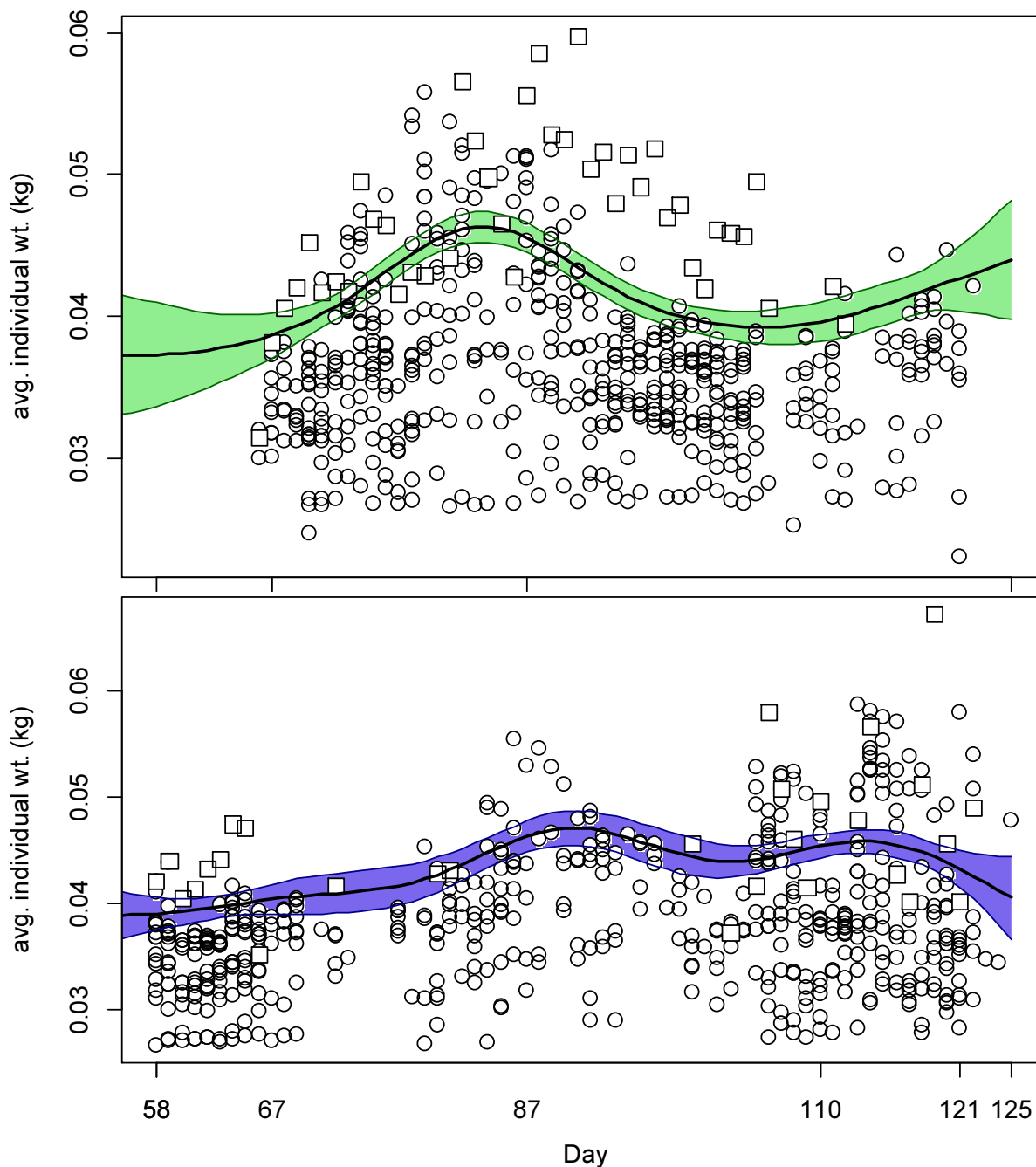


Figure A1. North (top) and south (bottom) sub-area daily average individual calamari weights from commercial size categories per vessel (circles) and observer measurements (squares). GAMs of the daily trends  $\pm$  95% confidence intervals (centre lines and colour under-shading).

To smooth fluctuations, generalized additive model (GAM) trends were calculated of daily average individual weights. North and south sub-areas were calculated separately. For continuity, the GAMs were calculated using all pre-season survey and in-season data contiguously. North and south GAMs were first calculated separately on the commercial and observer data. The commercial data GAMs were taken as the baseline trends, and calibrated

to the observer data GAMs in proportion to the correlation between the commercial data and observer data GAMs. For example, if the season average individual weight estimate from commercial data was 0.052 kg, the season average individual weight estimate from observer data was 0.060 kg, and the coefficient of determination ( $R^2$ ) between commercial and observer GAM trends was 86%, then the resulting trend of daily average individual weights was calculated as the commercial data GAM values +  $(0.060 - 0.052) \times 0.86$ . This way, both the greater day-to-day consistency of the commercial data trends, and the greater point value accuracy of the observer data are represented in the calculations. GAM plots of the north and south sub-areas are shown in Figure A1.

### Prior estimates and CV

The pre-season survey (Winter et al., 2017) had estimated Falkland calamari biomasses of 3,255 t (standard deviation:  $\pm 2,820$  t) north of  $52^\circ$  S and 45,529 t (standard deviation: 8,142 t) south of  $52^\circ$  S. From modelled survey catchability, Payá (2010) had estimated average net escapement of up to 22%, which was added to the standard deviation:

$$45,529 \pm \left( \frac{8,142}{45,529} + .22 \right) = 45,529 \pm 39.9\% = 45,529 \pm 18,159 \text{ t} \quad (\text{A1-S})$$

$$3,255 \pm \left( \frac{2,820}{3,255} + .22 \right) = 3,255 \pm 108.6\% = 3,255 \pm 3,536 \text{ t} \quad (\text{A1-N})$$

The 22% was added as a linear increase in the variability, but was not used to reduce the total estimate, because calamari that escape one trawl are likely to be part of the biomass concentration that is available to the next trawl.

In previous seasons, calamari numbers at the start of the commercial season were assumed equivalent to the survey that ended immediately prior. In this season, with a four-day postponement between the end of the survey (day 54) and the start of the commercial season (day 58), the gap was bridged by discounting the survey estimate at the rate of natural mortality (M) over four days, and implicitly assuming that no further immigrations of calamari occurred during those four days. This is computationally equivalent to season time series in which either the north or south sub-area only started to receive fishing effort some days after the start of the season (e.g., Winter 2015; 2016).

Calamari numbers at the end of the survey were estimated as the survey biomasses divided by the GAM-predicted individual weight averages for the survey: 0.0379 kg north, 0.0386 kg south (Figure A1), and 0.0397<sup>a</sup> kg combined. Average coefficients of variation (CV) of the GAM over the duration of the pre-season survey were 10.3% north and 7.1% south; and CV of the length-weight conversion relationship (Equation 7) were 6.7% north and 6.3% south. Combining these sources of variation with the pre-season survey biomass estimates and individual weight averages (above) gave estimated calamari numbers at survey end (day 54) of:

$$\text{prior } N_{S \text{ day } 54} = \frac{45,529 \times 1000}{0.0386} \pm \sqrt{39.9\%^2 + 4.6\%^2 + 6.3\%^2}$$

<sup>a</sup> Note that ‘combined’ is higher than either ‘north’ or ‘south’, rather than an intermediate between ‘north’ and ‘south’. As the ‘combined’ GAM is calculated independently, this is not a computational contradiction.

$$\begin{aligned}
&= 1.180 \times 10^9 \pm 40.6\% \\
\text{prior } N_{N \text{ day } 54} &= \frac{3,255 \times 1000}{0.0379} \pm \sqrt{108.6\%^2 + 6.1\%^2 + 6.7\%^2} \\
&= 0.086 \times 10^9 \pm 109.0\%
\end{aligned}$$

Priors were normalized for the combined fishing zone average, to produce better continuity as vessels fish sometimes north and sometimes south:

$$\begin{aligned}
\text{nprior } N_{S \text{ day } 54} &= \left( \frac{(3,255 + 45,529) \times 1000}{0.0397} \right) \times \left( \frac{\text{prior } N_{S \text{ day } 54}}{\text{prior } N_{N \text{ day } 54} + \text{prior } N_{S \text{ day } 54}} \right) \\
&= 1.147 \times 10^9 \pm 40.6\% \tag{A2-S}
\end{aligned}$$

$$\begin{aligned}
\text{nprior } N_{N \text{ day } 54} &= \left( \frac{(3,255 + 45,529) \times 1000}{0.0397} \right) \times \left( \frac{\text{prior } N_{N \text{ day } 54}}{\text{prior } N_{N \text{ day } 54} + \text{prior } N_{S \text{ day } 54}} \right) \\
&= 0.084 \times 10^9 \pm 109.0\% \tag{A2-N}
\end{aligned}$$

The catchability coefficient (q) prior for the south sub-area was taken on day 58, the first day of the season, when all 15 vessels that had entered the fishery were operating south. As noted, the prior of calamari numbers on day 58 was discounted for four days' mortality since the end of the survey:

$$\text{nprior } N_{S \text{ day } 58} = \text{nprior } N_{S \text{ day } 54} \times e^{-M \cdot (58-54)} - \text{CNMD}_{\text{day } 58} = 1.087 \times 10^9$$

where  $\text{CNMD}_{\text{day } 58} = 0$  as no catches had been taken between day 54 and day 58. Thus:

$$\begin{aligned}
\text{prior } q_S &= C(N)_{S \text{ day } 58} / (\text{nprior } N_{S \text{ day } 58} \times E_{S \text{ day } 58}) \\
&= (C(B)_{S \text{ day } 58} / \text{Wt}_{S \text{ day } 58}) / (\text{nprior } N_{S \text{ day } 58} \times E_{S \text{ day } 58}) \\
&= (861.4 \text{ t} / 0.0390 \text{ kg}) / (1.087 \times 10^9 \times 15 \text{ vessel-days}) \\
&= 1.355 \times 10^{-3} \text{ vessels}^{-1} \text{ b} \tag{A4-S}
\end{aligned}$$

CV of the prior was calculated as the sum of variability in  $\text{nprior } N_{S \text{ day } 54}$  (Equations A2-S) plus variability in the catches of vessels on the start day 58, plus variability of the natural mortality (see Appendix section Natural mortality, below):

$$\begin{aligned}
\text{CV}_{\text{prior } S} &= \sqrt{41.0\%^2 + \left( \frac{\text{SD}(C(B)_{S \text{ vessels day } 58})}{\text{mean}(C(B)_{S \text{ vessels day } 58})} \right)^2 + \left( 1 - \text{sign}(1 - \text{CV}_M) \times \text{abs}(1 - \text{CV}_M)^{(58-54)} \right)^2} \\
&= \sqrt{40.6\%^2 + 31.5\%^2 + 48.9\%^2} = 71.0\% \tag{A5-S}
\end{aligned}$$

<sup>b</sup> On Figure 6-left.

The catchability coefficient ( $q$ ) prior for the north sub-area was calculated on day 67, when 9 vessels first fished north and the initial depletion period north started. The prior of calamari numbers on day 58 was discounted for natural mortality over the days since the end of the survey:

$${}_{\text{nprior}}N_{\text{N day 67}} = {}_{\text{nprior}}N_{\text{N day 54}} \times e^{-M \cdot (67-54)} - \text{CNMD}_{\text{day 67}} = 0.069 \times 10^9 \quad (\text{A3-N})$$

where  $\text{CNMD}_{\text{day 67}} = 0$  as no catches had been taken between day 54 and day 67. This calculation was inadequate, however, as it equated to a negative number of calamari, given the catch rate, by the day before the next immigration in the north sub-area (day 86):

$${}_{\text{nprior}}N_{\text{N day 86}} = {}_{\text{nprior}}N_{\text{N day 67}} \times e^{-M \cdot (86-67)} - \text{CNMD}_{\text{day 86}} = -0.133 \times 10^9$$

By default, it was assumed instead that the number of calamari on day 67 must have been high enough to reduce the absolute count on day 86 to no less than two:

$${}_{\text{min}}N_{\text{N day 67}} = 2 + \text{CNMD}_{\text{day 86}} / e^{-M \cdot (86-67)} = 0.240 \times 10^9$$

Thus:

$$\begin{aligned} \text{prior } q_{\text{N}} &= C(\text{N})_{\text{N day 67}} / ({}_{\text{nprior}}N_{\text{N day 67}} \times E_{\text{N day 67}}) \\ &= (C(\text{B})_{\text{N day 67}} / \text{Wt}_{\text{N day 67}}) / ({}_{\text{nprior}}N_{\text{N day 67}} \times E_{\text{N day 67}}) \\ &= (464.9 \text{ t} / 0.0387 \text{ kg}) / (0.240 \times 10^9 \times 6 \text{ vessel-days}) \\ &= 5.563 \times 10^{-3} \text{ vessels}^{-1} \end{aligned}$$

This  $q$  value was found to be implausibly high. The difficulty of determining a realistic  $q$  value, together with the very low calamari biomass found north during the survey (Winter et al. 2017), gave evidence that a new immigration likely occurred between days 54 and 67. As this putative immigration was apprehended by neither the survey nor commercial fishing, calculation of a  $q$  value from north data is effectively void. Instead, the same  $q$  prior as the south was used, based on the principle that in a Bayesian analysis unavailable prior data values can be ‘borrowed’ from comparable data sets (Su et al. 2001, Jiao et al 2011). Thus:

$$\text{prior } q_{\text{N}} = \text{prior } q_{\text{S}} = 1.355 \times 10^{-3} \text{ vessels}^{-1} \text{ }^c \quad (\text{A4-N})$$

$$\text{CV}_{\text{prior N}} = \text{CV}_{\text{prior S}} = 71.0\% \quad (\text{A5-N})$$

### Depletion model estimates and CV

For the south sub-area, the equivalent of Equation 2 with three  $N_{\text{day}}$  was optimized on the difference between predicted catches and actual catches (Equation 3), resulting in parameters values:

$$\begin{aligned} \text{depletion } N_{1\text{S day 58}} &= 4.639 \times 10^6; & \text{depletion } N_{2\text{S day 110}} &= 0.701 \times 10^6 \\ \text{depletion } N_{3\text{S day 121}} &= 0.519 \times 10^6 \end{aligned}$$

<sup>c</sup> On Figure 8-left.

$$\text{depletion } Q_S = 2.620 \times 10^{-10} \text{ d} \quad (\text{A6-S})$$

The normalized root-mean-square deviation of predicted vs. actual catches was calculated as the CV of the model:

$$\begin{aligned} CV_{\text{rmsd } S} &= \frac{\sqrt{\sum_{i=1}^n \left( \text{predicted } C(N)_{S \text{ day } i} - \text{actual } C(N)_{S \text{ day } i} \right)^2 / n}}{\text{mean}(\text{actual } C(N)_{S \text{ day } i})} \\ &= 2.105 \times 10^6 / 7.329 \times 10^6 = 28.7\% \end{aligned} \quad (\text{A7-S})$$

$CV_{\text{rmsd } S}$  was added to the variability of the GAM-predicted individual weight averages for the season (Figure A1-S); equal to a CV of 1.9% south. CVs of the depletion were then calculated as the sum:

$$\begin{aligned} CV_{\text{depletion } S} &= \sqrt{CV_{\text{rmsd } S}^2 + CV_{\text{GAM Wt } S}^2} = \sqrt{28.7\%^2 + 1.9\%^2} \\ &= 28.8\% \end{aligned} \quad (\text{A8-S})$$

For the north sub-area, the equivalent of Equation 2 with two  $N_{\text{day}}$  was optimized on the difference between predicted catches and actual catches (Equation 3), resulting in parameters values:

$$\begin{aligned} \text{depletion } N1_{N \text{ day } 67} &= 0.989 \times 10^9; & \text{depletion } N2_{N \text{ day } 87} &= 0.299 \times 10^9 \\ \text{depletion } Q_N &= 1.315 \times 10^{-3} \text{ e} \end{aligned} \quad (\text{A6-N})$$

The root-mean-square deviation of predicted vs. actual catches was calculated as the CV of the model:

$$\begin{aligned} CV_{\text{rmsd } N} &= \frac{\sqrt{\sum_{i=1}^n \left( \text{predicted } C(N)_{N \text{ day } i} - \text{actual } C(N)_{N \text{ day } i} \right)^2 / n}}{\text{mean}(\text{actual } C(N)_{N \text{ day } i})} \\ &= 1.906 \times 10^6 / 8.567 \times 10^6 = 22.2\% \end{aligned} \quad (\text{A7-N})$$

$CV_{\text{rmsd } N}$  was added to the variability of the GAM-predicted individual weight averages for the season (Figure A1-N); equal to a CV of 1.4% north. CVs of the depletion were then calculated as the sum:

$$\begin{aligned} CV_{\text{depletion } N} &= \sqrt{CV_{\text{rmsd } N}^2 + CV_{\text{GAM Wt } N}^2} = \sqrt{22.2\%^2 + 1.4\%^2} \\ &= 22.3\% \end{aligned} \quad (\text{A8-N})$$

<sup>d</sup> On Figure 6-left.

<sup>e</sup> On Figure 8-left.

### Combined Bayesian models

For the south sub-area, the joint optimization of Equations 3 and 4 resulted in parameters values:

$$\begin{aligned}
 \text{Bayesian } N1_S \text{ day 58} &= 1.480 \times 10^9; & \text{Bayesian } N2_S \text{ day 110} &= 0.323 \times 10^9 \\
 \text{Bayesian } N3_S \text{ day 121} &= 0.200 \times 10^9 \\
 \text{Bayesian } Q_S &= 1.005 \times 10^{-3} \text{ }^f & & \text{(A9-S)}
 \end{aligned}$$

These parameters produced the fit between predicted catches and actual catches shown in Figure A2-S.

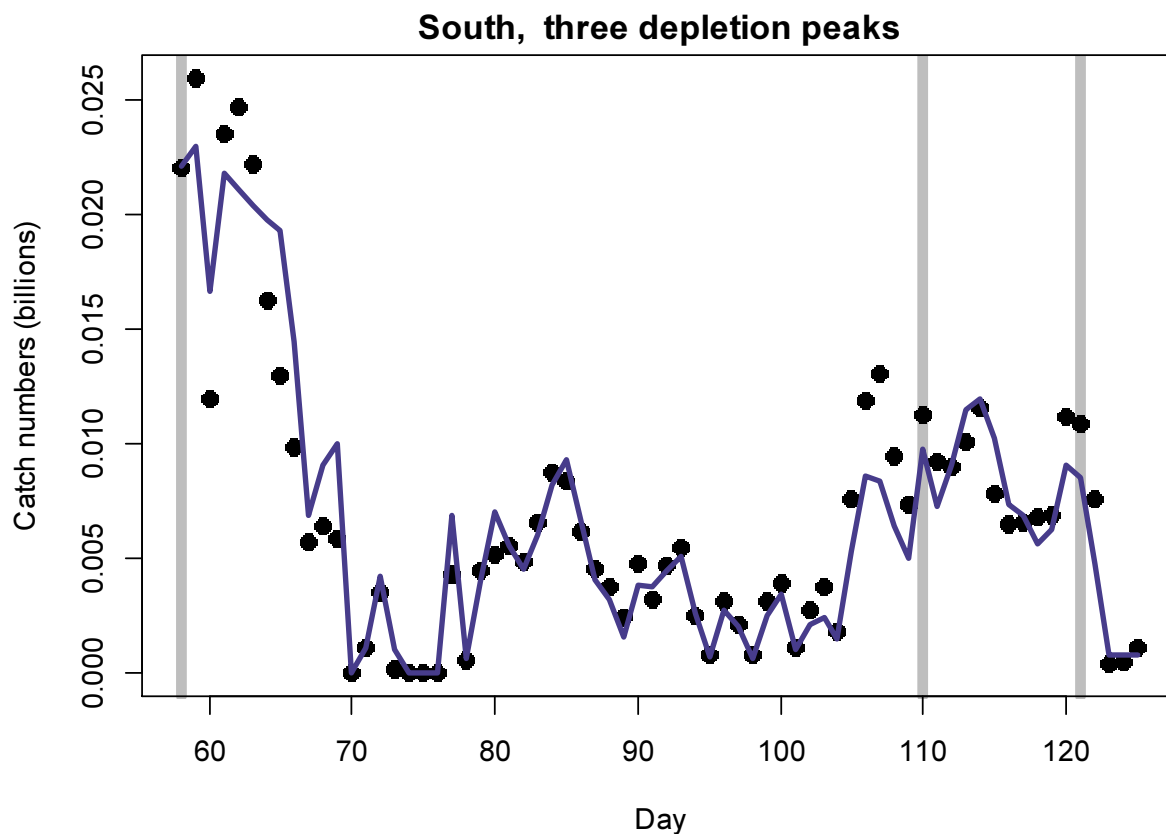


Figure A2-S. Daily catch numbers estimated from actual catch (black points) and predicted from the depletion model (blue line) in the south sub-area.

For the north sub-area, joint optimization of Equations 3 and 4 resulted in parameters values:

$$\begin{aligned}
 \text{Bayesian } N1_N \text{ day 67} &= 0.971 \times 10^9; & \text{Bayesian } N2_N \text{ day 87} &= 0.298 \times 10^9 \\
 \text{Bayesian } Q_N &= 1.343 \times 10^{-3} \text{ }^g & & \text{(A9-N)}
 \end{aligned}$$

These parameters produced the fit between predicted catches and actual catches shown in Figure A2-N.

<sup>f</sup> On Figure 6-left.

<sup>g</sup> On Figure 8-left.

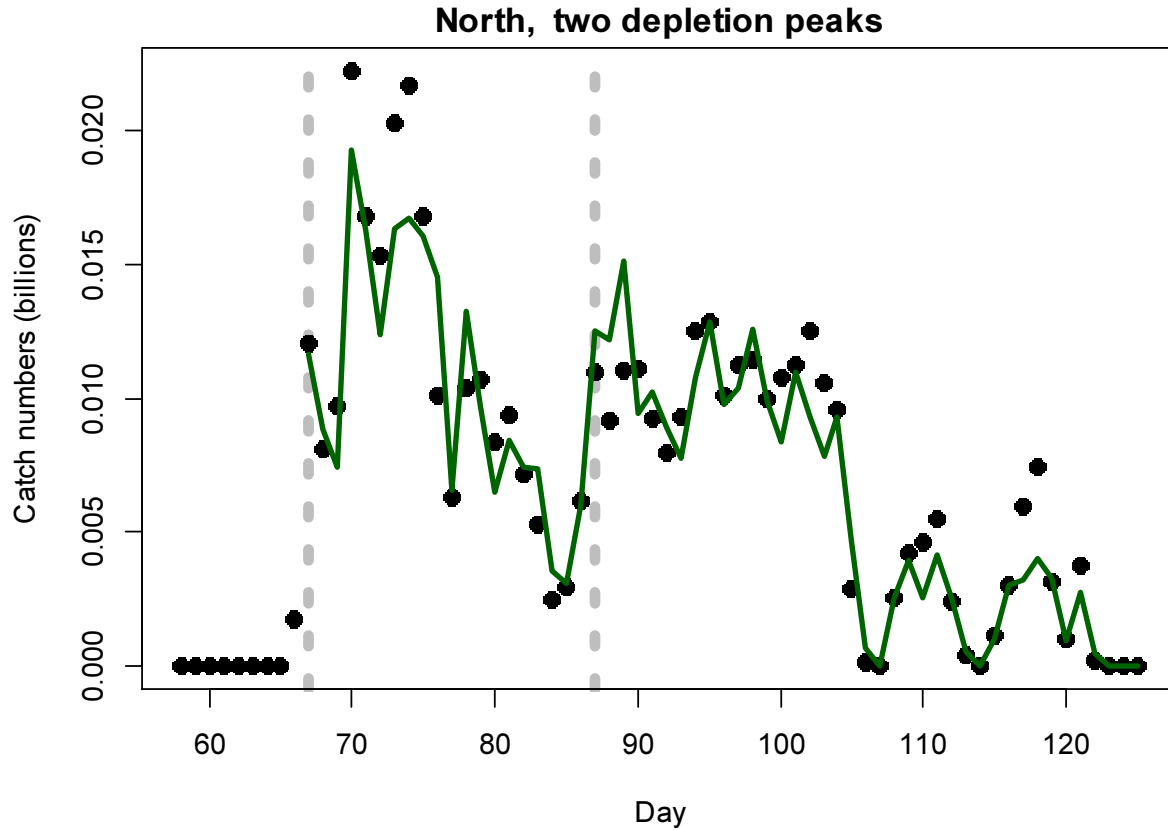


Figure A2-N. Daily catch numbers estimated from actual catch (black points) and predicted from the depletion model (green line) in the north sub-area.

### Natural mortality

Natural mortality is parameterized as a constant instantaneous rate  $M = 0.0133 \text{ day}^{-1}$  (Roa-Ureta and Arkhipkin, 2007), based on Hoenig’s (1983) log mortality vs. log maximum age regression applied to an estimated maximum age of 352 days for *Doryteuthis gahi*:

$$\begin{aligned}
 \log(M) &= 1.44 - 0.982 \times \log(\text{age}_{\max}) \\
 M &= \exp(1.44 - 0.982 \times \log(352)) \\
 &= 0.0133
 \end{aligned}
 \tag{A10}$$

The parameterization  $M = 0.0133 \text{ day}^{-1}$  is used in the current assessment. However, the adjustment required for the scheduled postponement of this season brought focus on the process uncertainty of the natural mortality estimate. Hoenig (1983) derived Equation **A10** from the regression of 134 stocks among 79 species of fish, molluscs, and cetaceans. Hoenig’s regression obtained  $R^2 = 0.82$ , but a corresponding coefficient of variation (CV) was not published. Therefore, a CV of  $M$  was estimated for the current assessment by measuring the coordinates off a print of Figure 1 in Hoenig (1983) and repeating the regression. Variability of  $M$  was calculated by randomly re-sampling, with replacement, the regression coordinates 10000 $\times$  and re-computing Equation **A10** for each iteration of the

resample. The resulting variability distribution of M is shown in Figure A3. The CV of M from the 10000 random resamples was:

$$CV_M = SD_M / Mean_M$$

$$CV_M = 0.0021 / 0.0134 = 15.46\% \quad (\text{A11})$$

$CV_M$  over the aggregate number of unassessed days was then added to the CV of the biomass prior estimate and the CV of variability in vessel catches on start day (A5-S).  $CV_M$  was further expressed as an absolute value and indexed by  $\text{sign}(1 - CV_M)$  to ensure that the value could not decrease if  $CV_M$  was hypothetically  $> 100\%$  (A5-S).

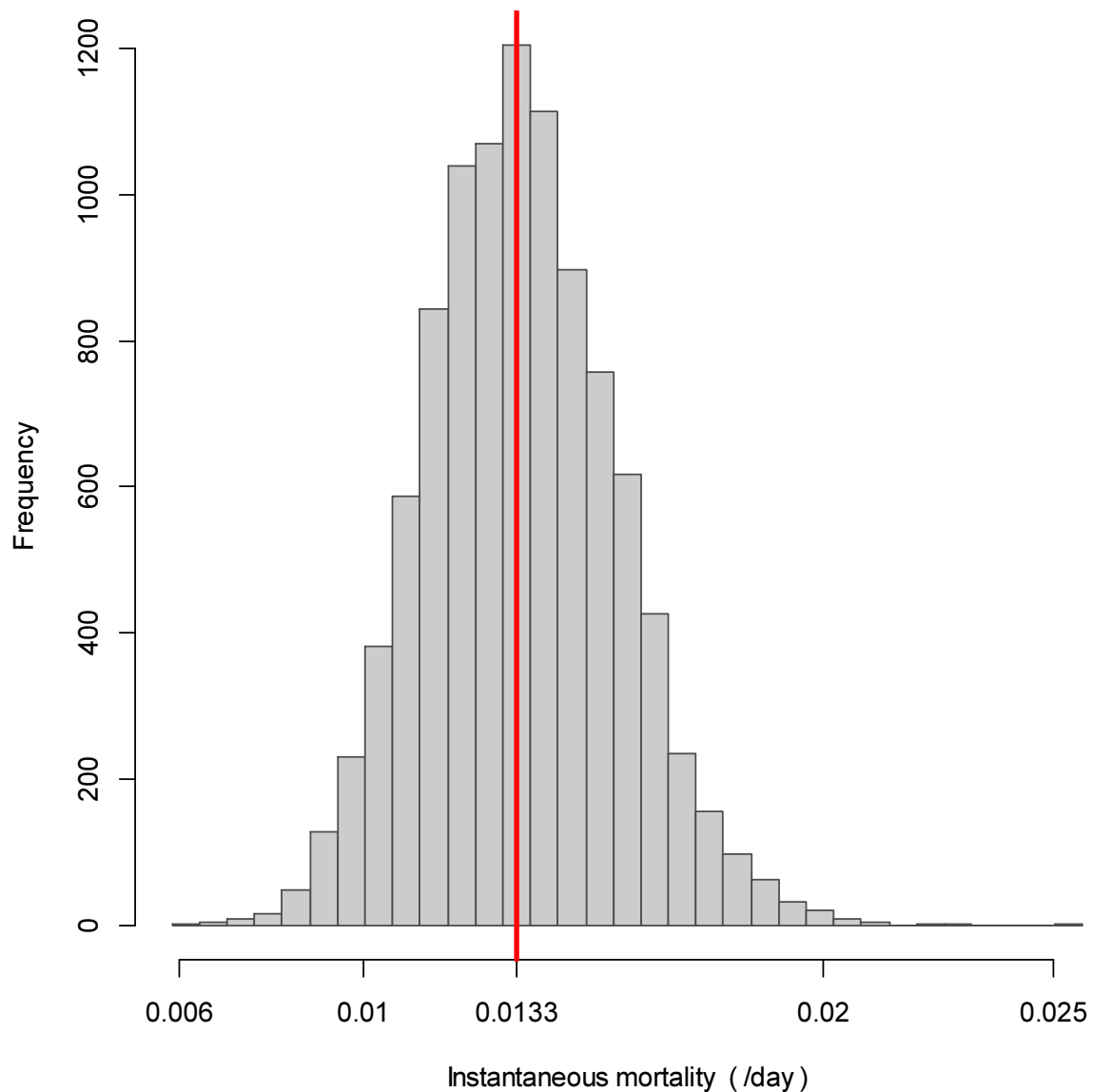


Figure A3. Variability distribution of the instantaneous natural mortality M from randomly re-sampling Hoenig's (1983) regression of log mortality vs. log maximum age.

## Total catch by species

Table A1: Total reported catches and discard by taxon during first season 2017 calamari fishing, and number of catch reports in which each taxon occurred.

Species Code	Species / Taxon	Catch Wt. (KG)	Discard Wt. (KG)	N Reports
LOL	<i>Doryteuthis gahi</i>	39433312	4225	997
PAR	<i>Patagonotothen ramsayi</i>	687259	677112	960
MUN	<i>Munida</i> spp.	78071	78071	171
BAC	<i>Salilota australis</i>	50186	2947	182
CGO	<i>Cottoperca gobio</i>	17740	17299	468
ILL	<i>Illex argentinus</i>	17055	10113	267
HAK	<i>Merluccius hubbsi</i>	10112	3652	211
PTE	<i>Patagonotothen tessellata</i>	9020	9020	86
TOO	<i>Dissostichus eleginoides</i>	8816	1749	161
RAY	Rajidae	8418	6302	307
KIN	<i>Genypterus blacodes</i>	6719	2822	124
BLU	<i>Micromesistius australis</i>	6522	6522	19
ALF	<i>Allothunnus fallai</i>	3456	3444	168
SCA	scallop	2970	2970	75
WHI	<i>Macruronus magellanicus</i>	1446	1110	23
ING	<i>Moroteuthis ingens</i>	1040	1040	94
OCT	Octopus spp.	875	875	46
CHE	<i>Champocephalus esox</i>	831	777	95
CAV	<i>Campylonotus vagans</i>	720	720	4
DGS	<i>Squalus acanthias</i>	488	488	37
POR	<i>Lamna nasus</i>	476	476	7
DGH	<i>Schroederichthys bivius</i>	460	460	37
MED	Medusae sp.	388	388	15
GRV	<i>Macrourus</i> spp.	372	372	20
PAT	<i>Merluccius australis</i>	183	183	8
EEL	<i>Iluocoetes fimbriatus</i>	59	59	10
CAM	<i>Cataetyx messieri</i>	41	41	6
MAR	<i>Martialia hyadesi</i>	34	34	1
BDU	<i>Brama dussumieri</i>	34	34	5
SPN	Porifera	33	33	4
RED	<i>Sebastes oculatus</i>	22	22	5
BUT	<i>Stromateus brasiliensis</i>	22	22	13
SEP	<i>Seriolaella porosa</i>	13	13	3
DGX	dogfish / catshark uid	11	11	2
MYX	<i>Myxine</i> spp.	9	9	4
MUL	<i>Eleginops maclovinus</i>	5	5	1
OTH		5	5	2
NEM	<i>Neophrnichthys marmoratus</i>	2	2	2
COP	<i>Congiopodus peruvianus</i>	1	1	1
Total		40347226	833428	997